TECTONICS, VOL. 13, NO. 4, PAGES 837-857, AUGUST 1994

Cooling history of the northern Ford Ranges, Marie Byrd Land, West Antarctica

S. M. Richard,[1,2] C. H. Smith,[1,3] D. L. Kimbrough,[4] P. G. Fitzgerald,[5]
B. P. Luyendyk,[1] and M. O. McWilliams[6]

Abstract. Thermochronologic data from the Fosdick, Phillips and Chester mountains of Marie Byrd Land, West Antarctica, have been obtained through U-Pb analysis of monazite, $^{40}Ar/^{39}Ar$ analysis of hornblende, muscovite, biotite and K-feldspar, and apatite fission track methods. These data were collected to test the hypothesis that high-grade metamorphic rocks in the Fosdick Mountains occupy the footwall of a Cordilleran-style metamorphic core complex, exhumed during the breakup of this sector of Gondwana in early Late Cretaceous time. High-grade metamorphism of rocks exposed in the Fosdick Mountains was followed by rapid cooling starting at ~105 Ma, during the transition from convergence to extension in the adjacent continental margin of Gondwana. Monazite, hornblende, muscovite, biotite, and K-feldspar from the Fosdick Mountains record rapid cooling (70 ± 30°C/m.y.) from peak metamorphic conditions of 725°-780°C at 4.3-5.6 kbar to below 165°C between 105 and 94 Ma. Subsequent slow cooling was apparently punctuated by a short period of accelerated cooling through the apatite partial annealing zone (~110°-60°C) between ~80 and 75 Ma. Cooling rates decreased to an average of ~1°C/m.y. after 70 Ma. Cooling ages become progressively older to the south; metamorphic grade decreases in concert with the increasing cooling ages. The southernmost samples, from the Chester Mountains, probably cooled to below K-feldspar closure temperature (~165°C) before inferred reheating associated with metamorphism in the Fosdick Mountains. North of the Fosdick Mountains, Devonian Ford granodiorite in the Phillips Mountains was below K-feldspar closure temperature by early Cretaceous time. Byrd Coast granite intrusions in the eastern Phillips Mountains and east of the Fosdick and Chester mountains were emplaced between 100 and 105 Ma, and these plutons cooled very rapidly (>100°C/m.y.) to below biotite closure temperature, consistent with their epizonal character. The relationship of these granitoids to metamorphic rocks in the Fosdick Mountains is uncertain. We hypothesized the following sequence of events during the transition from convergence to extension along the Pacific margin of Gondwana. Voluminous intrusion into the lower and middle crust led to increased heat flow and high-temperature, low- to moderate-pressure metamorphism, forming the Fosdick metamorphic complex (FMC) exposed in the Fosdick Mountains. Decrease in strength due to intrusion and partial melting resulted in large-scale flow, probably driven by extension-related differential stresses. This deformation ended before the onset of rapid cooling of the FMC at ~105 Ma. Cooling rates determined for the FMC can be modeled by decreasing the heat flux into the crust and exhuming the complex at a rate of 1.5 mm/yr. The decrease in cooling rate between closure of K-feldspar $^{40}Ar/^{39}Ar$ at ~94 Ma and cooling into the apatite fission track partial annealing zone by ~80 Ma is interpreted to indicate that exhumation was at least a two-stage process. Our observations indicate that the Fosdick and Chester mountains are part of a coherent block that was tilted ~20° to the south during the exhumation of the FMC, probably by movement along an east trending, north dipping, normal fault between the Fosdick and Phillips mountains. The Fosdick Mountains are not a Cordillcran-style metamorphic core complex, but the FMC provides a record of middle-crustal processes related to the rifting of New Zealand from Gondwana in the Late Cretaceous.

Introduction

The Fosdick Mountains, located in the northern part of the Ford Ranges of Marie Byrd Land (Figure 1), are formed of metasedimentary and metaplutonic rocks, included in the Fosdick metamorphic complex (FMC) [*Smith*, 1992]. These rocks have been metamorphosed to much higher-grade metamorphic conditions than rocks in surrounding ranges. Rocks in the Fosdick Mountains were first described by members of the Byrd Coastal Survey, who visited the northern Ford Ranges during 1966-1967 and produced the first geologic maps of the region. The results of their study are presented in a series of 1:250,000-scale geologic maps [*Wade et al.*, 1977a, b, c, 1978] and several papers [*Klimov*, 1967; *Wade and Wilbanks*, 1972; *Lopatin and Orlenko*, 1972]. The contrast between the high-grade metamorphic rocks of the Fosdick Mountains and low-grade metasedimentary rocks and associated plutons found in adjacent ranges led to more detailed study of the Fosdick Mountains by *Wilbanks* [1969, 1972]. He recognized two periods of metamorphism and deformation based on mineral textures and fold-hinge orientation and migmatization that accompanied and partly postdated the younger folding event. *Wilbanks* [1972] proposed an "infrastructure-superstructure" relationship between the high grade rocks of the Fosdick Mountains and the low-grade metasedimentary rocks in adja-

[1]Institute for Crustal Studies, University of California, Santa Barbara.
[2]Now at Arizona Geological Survey, Tucson.
[3]Now at Geology Dept., Colorado College, Colorado Springs.
[4]Dept. of Geological Sciences, San Diego State University, San Diego, California.
[5]Geosciences Department, University of Arizona, Tucson.
[6]Dept. of Geophysics, Stanford University, Stanford, California.

Paper number 93TC03322.
0278-7407/94/93TC-03322$10.00

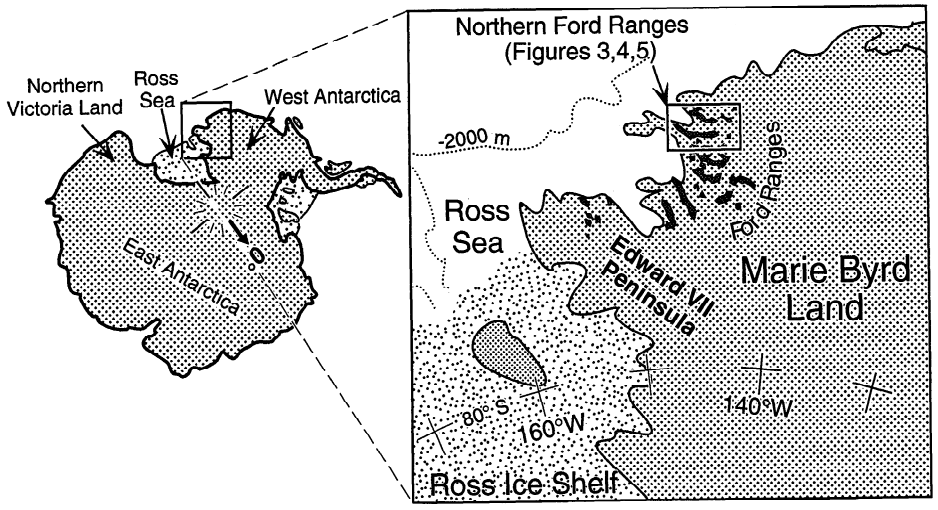

Figure 1. Map showing location of Fosdick Mountains, Ford Ranges, and other locations referred to in text.

cent ranges, which he compared with that described in East Greenland [*Haller*, 1971].

The 1978-1979 New Zealand expedition [*Adams et al.*, 1989] traveled throughout the southern Ford Ranges and visited the southernmost rock outcrops in the Fosdick Mountains. Field relationships and details of sedimentary composition led them to interpret paragneiss in the FMC as a high grade equivalent of the low-grade metasediments that are widespread in the southern Ford Ranges [*Bradshaw et al.*, 1983; *Adams*, 1986]. On the basis of Rb-Sr data, *Halpern* [1968, 1972] and *Adams* [1986] suggested that high-grade metamorphism in the Fosdick Mountains was Cretaceous in age.

These observations from Antarctica and the recognition of Cretaceous metamorphic core complexes in New Zealand, believed to be related to the Cretaceous rifting of New Zealand from Gondwana [*Gibson et al.*, 1988; *Tulloch and Kimbrough*, 1989], suggested the possibility that the Ford Ranges were a basin-and-range-style extended terrane [e.g., *Davis and Lister*, 1988]. To test the hypothesis that rocks of widely differing metamorphic grade in adjacent ranges are juxtaposed across a large, low-angle normal or detachment fault, we visited the northern Ford Ranges (Figure 1) during the 1989-1990 and 1990-1991 field seasons. This paper summarizes the thermochronology of the Fosdick Mountains area.

Geologic Setting

Scattered bedrock outcrops in West Antarctica are grouped into several terranes that formed the Pacific margin of Gondwana between what is now South America and Australia in early Cretaceous time [*Storey et al.*, 1988; *Dalziel and Elliot*, 1982; *Dalziel and Grunow*, 1985] (Figure 2). The Marie Byrd Land crustal block is the westernmost of these terranes and lies adjacent to the Ross Sea. This block shared a history of early Paleozoic deepwater sedimentation and Devonian-Carboniferous plutonism with the Robertson Bay terrane of northern Victoria Land, the Stalwell terrane of Australia, and the Buller terrane in New Zealand [*Wade and Couch*, 1982; *Bradshaw et al.*, 1983; *Adams*, 1986; *Stump et al.*, 1986; *Borg and DePaolo*, 1991; *Weaver et al.*, 1991]. *Borg and DePaolo* [1991] propose that northern Victoria Land and Marie Byrd Land were intruded by Devonian-Early Carboniferous plutons in a region remote from East Antarctica and accreted to Gondwana between latest Devonian and Permian time (see also *Weaver et al.* [1991]).

During Middle Jurassic to late Early Cretaceous time an active margin of Gondwana was continuous from New Zealand, through West Antarctica and the Antarctic Peninsula, to southern South America (Figure 2) [*Cooper et al.*, 1982; *Dalziel et al.*, 1987]. Rapid uplift and cooling of high-grade metamorphic rocks is documented along this margin of Gondwana between 120 and ~100 Ma in New Zealand [*J. Y. Bradshaw*, 1989; *Mattinson et al.*, 1986; *Tulloch and Kimbrough*, 1989] and between ~85 and 65 Ma in southern South America [*Mukasa et al.*, 1988; *Dalziel and Brown*, 1989]. On the basis of geologic arguments, *J. D. Bradshaw* [1989] proposed that the transition from convergent to extensional tectonic regime at ~105 Ma in New Zealand resulted from oblique subduction of a Pacific-Phoenix spreading center from west to east along the Pacific margin of Gondwana. Subduction along the Pacific margin of the Antarctic Peninsula and South America continued into late Cenozoic time, as the Pacific-Aluk ridge, perhaps a relict of the proposed Pacific-Phoenix ridge, was subducted obliquely from west to east along this margin [*Mayes et al.*, 1990].

In the reconstruction of *Grindley and Davey* [1982], initial separation of the Campbell Plateau from New Zealand and Marie Byrd Land occurred along a system of right-slip faults between Antarctica and the Australia-New Zealand block during Cretaceous time. *Bradshaw* [1991] interpreted the margin of the Campbell Plateau as a broad right-lateral transtensional zone at the time of rifting. Other systems of strike-slip faults active during the Jurassic-Cretaceous breakup stage have been proposed between East and West Antarctica [*Lawver et al.*, 1985; *Dalziel et al.*, 1987; *Lawver and Gahagan*, 1991]. Oceanic crust was present between the Campbell Plateau and Marie Byrd Land by the time of anomaly 34 (84 Ma) [*Cande and Mutter*, 1982; *Kamp*, 1986; *Mayes et al.*, 1990]. Reconstruction of the West Antarctica-New Zealand-Australia-South America section of Gondwana typically results in significant overlap of crustal blocks, which is resolved if internal exten-

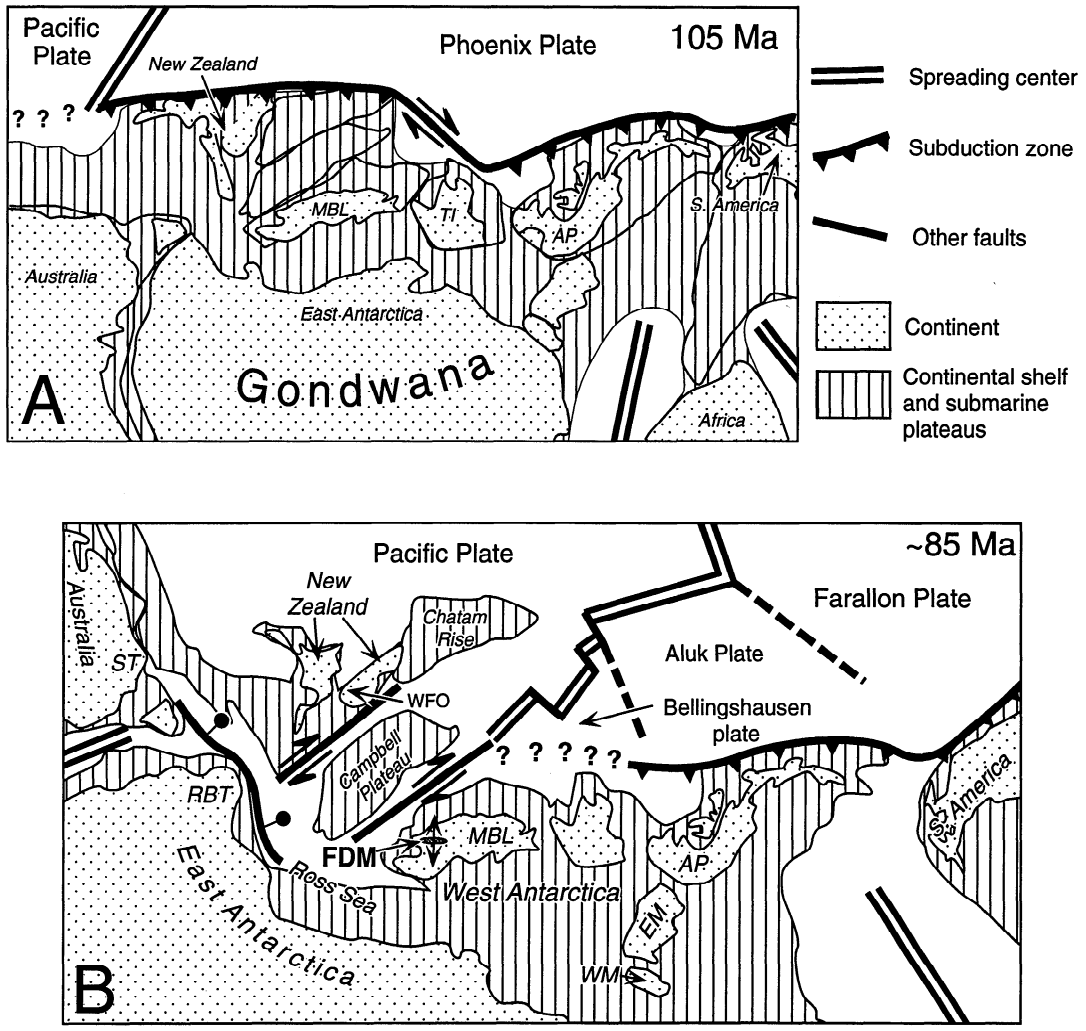

Figure 2. Map of the Pacific Margin of Gondwana showing terranes of West Antarctica and their proposed relationship to South America and New Zealand in Cretaceous time. (a) Setting is at ~105 Ma; the Pacific-Phoenix ridge intersects the trench obliquely. As it was consumed, subduction ceased along the New Zealand margin of Gondwana. Strongly oblique convergence probably occurred along Chatham Rise-Thurston Island segment of Gondwana Margin. Map is based on works by *J. D. Bradshaw* [1989], *Lawver and Scotese* [1987], *Lawver et al.* [1991], and *DeWit* [1990]. The relationship between Antarctic Peninsula, South America and Africa is schematic. (b) Setting is at ~85 Ma. The Campbell Plateau has rifted from Marie Byrd Land, while subduction continues along the Antarctic Peninsula. The area of Chatham Rise, Campbell Plateau and Marie Byrd Land has increased due to extension during rifting [cf. *Bradshaw*, 1991]. The relationship of the Pacific-Aluk ridge to the proposed Pacific-Phoenix ridge is unknown. Map is based on works by *Grindley and Davey* [1982] and *Mayes et al.* [1990]. Abbreviations are: AP, Antarctic Peninsula; EM, Ellsworth Mountains block; FDM, Fosdick Mountains; MBL, Marie Byrd Land crustal block; RBT, Robertson Bay Terrane; ST, Stalwell terrane, Australia; TI, Thurston Island; WFO, western Fiordland Orthogneiss; and WM, Whitmore Mountains block. Areas with no pattern are oceanic crust.

sion of these blocks is restored [*Cooper et al.*, 1982; *Storey et al.*, 1988; *Kamp and Fitzgerald*, 1987; *Bradshaw*, 1991]. The Campbell Plateau, for example, may be at least 200 km wider at present than it was in Early Cretaceous time [*Bradshaw*, 1991].

Geology of Northern Ford Ranges

Most of the Ford Ranges (Figure 1) are underlain by low-grade metasedimentary rocks of the pre-Late Ordovician Swanson Formation, intruded by Devonian Ford granodiorite and Cretaceous Byrd Coast granite [*Wade et al.*, 1977a, b, c, 1978; *Adams*, 1986, 1987]. The Swanson Formation includes an uncertain thickness of alternating sandstone and mudstone deposited as deep marine turbidites. Whole rock K-Ar and Rb-Sr data from these cleaved, subgreenschist facies slates cluster around 450 Ma. Rb-Sr isochron ages and biotite cooling ages for the Ford granodiorite from several areas in the Ford Ranges cluster between 355 and 375 Ma [*Adams*, 1987]. U-Pb analysis of zircons from Ford granodiorite in the Chester Mountains

yielded an age of 353 Ma [*Richard and Kimbrough*, 1991]. A second generation of granitoids, referred to as Byrd Coast granite [*Wade*, 1977a, b, c; *Adams*, 1987; *Weaver et al.*, 1991] intrudes Swanson Formation and Ford granodiorite in the Ford Ranges. Granitoids included in the Byrd Coast granite are typically leucocratic, but available chemical data indicate the presence of plutonic complexes ranging from calc-alkaline to peralkaline. Most are peraluminous, and both I-type and A-type granitoids have been included in this unit [*Weaver et al.*, 1991, 1992]. Relatively thin contact metamorphic aureoles associated with Byrd Coast granite plutons and igneous textures within them are consistent with emplacement at shallow crustal levels. No structural evidence for a Cretaceous crustal thickening event like that described in southern New Zealand [*J. Y. Bradshaw*, 1989] has been recognized in Marie Byrd Land.

Structural and Metamorphic History of the Fosdick Mountains

The Fosdick Mountains (145°W, 76°S) are an east-west trending mountain range located in the northern part of the Ford Ranges (Figures 1 and 3). They are underlain by high-grade metamorphic rocks referred to here as the Fosdick Metamorphic Complex (FMC), which are unique in the Ford Ranges. The FMC consists of two major components; unit 1, an older complex that includes paragneiss (derived from Swanson Formation?) intruded by monzogranite to granodiorite plutons, and unit 2, a series of synmetamorphic orthogneisses ranging from diorite to leucogranite.

Three fabrics related to high temperature deformational events are recognized in the FMC. The oldest fabric (S_1) is apparent only in sillimanite inclusions within garnet and cordierite porphyroblasts (C. H. Smith, manuscript in preparation, 1993). In unit 1 rocks, the second major deformational event (D_2) produced a steeply dipping gneissic foliation (S_2), most prominently displayed in the north-central part of the complex. S_2 was extensively transposed and locally obliterated during a subsequent event (D_3), which produced gently to moderately south-dipping, relatively planar gneissic layering (S_3), prominent in the eastern part of the complex. S_2 has no expression in unit 2 rocks, which were emplaced during D_3. Dense packets of aligned sillimanite inclusions that define S_1, are crenulated with hinge surfaces parallel to S_2 and overgrown by garnet or cordierite. Cordierite porphyroblasts are flattened parallel to S_2. Fattened cordierite porphyroblasts, along with included, crenulated sillimanite, are folded in D_3 folds [*Smith*, 1992].

The eastern and southern, structurally higher part of the FMC is characterized by relatively homogeneous, gently SE to south dipping S_3 gneissic foliation (Figure 3). This part of the complex consists mostly of unit 2 diorite to leucogranite

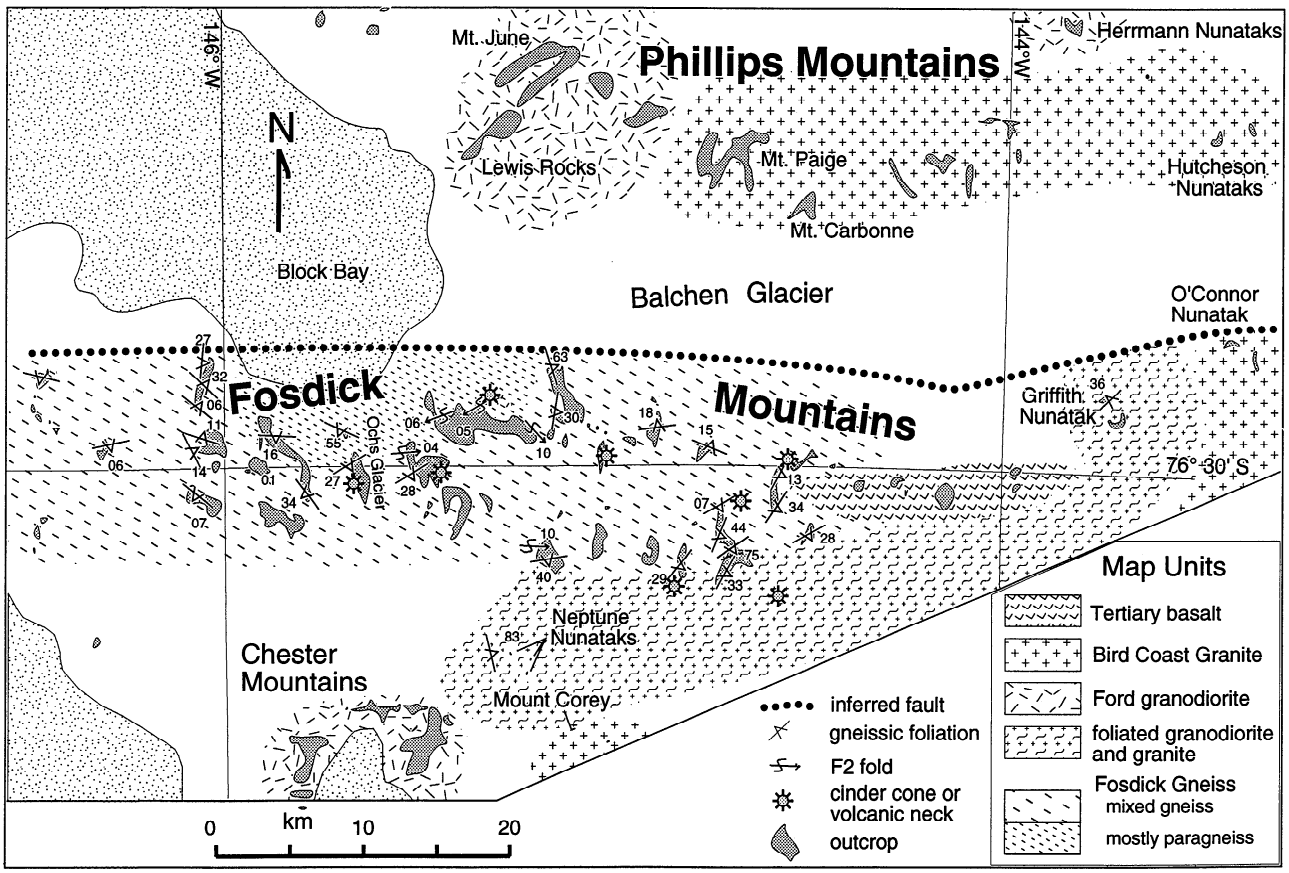

Figure 3. Geologic map of the Fosdick Mountains area based on fieldwork during 1989-1990 and 1990-1991 seasons [*Kimbrough et al.*, 1990; *Luyendyk et al.*, 1991]. Base map is from *Wade et al.* [1977c, 1978]. The limits of rock unit distribution are schematic.

orthogneisses that form a sill-like composite intrusion exceeding 2000 m in exposed thickness perpendicular to S_3. Individual sills are 5-30 m thick, separated by laterally continuous sheets of migmatitic paragneiss and orthogneiss. The large-scale lithologic layering and gneissic foliation within the sills define the S_3 foliation. Unit 2 orthogneisses show no evidence of polyphase fabrics and are typically nonmigmatitic, whereas older orthogneisses of unit 1 are migmatitic and contain S_2 foliation overprinted by S_3. Dioritic components of unit 2 are typically broken into large blocks and separated by leucocratic neosome (agmatite). The largest and most continuous unit 2 intrusions consist of garnet granodiorite to monzogranite. The composition of the diorite to monzogranite components of unit 2 is not compatible with partial melting within the exposed part of the complex, and these are interpreted to have been intruded early in the D_3 episode. Leucogranite sheets within the sill complex are interpreted to be locally derived anatectic granite because their mineralogy varies according to their host rocks. The present sill-like geometry unit 2 orthogneiss bodies probably resulted in part from D_3 deformation.

The central northern and western part of the FMC consists of mostly metapelitic gneiss (unit 1). A structural thickness of ~1000 m is exposed, measured normal to the S_3 foliation. D_3 shear zones bound lozenges of rock in which the D_2 foliation is preserved, and unit 2 granitoids form sills within these shear zones. The granitoids also form irregular bodies with diffuse boundaries, discordant to both S_2 and S_3, which consist of blocks of unit 1 and early unit 2 gneisses immersed in a nebulitic K-feldspar-porphyroblastic granitoid matrix. The gneissic foliation in the matrix of these "block gneisses" parallels the margins of the blocks. The block gneisses clearly postdate D_3 and are interpreted to represent coalesced bodies of anatectic granitoid in the process of mobilizing. In summary, the FMC is interpreted to represent a large-scale shear zone developed under high-grade metamorphic conditions. Zones of relatively straight S_3 foliation are interpreted to represent high-strain zones, in which the S_2 foliation has been obliterated by deformation and intrusion of unit 2 granitoid.

Mafic dikes were intruded continuously throughout the metamorphism and deformation of the Fosdick complex. The least deformed, youngest dikes are steeply dipping, fine-grained hornblende diorite and cut gneissic foliation; older dikes are buckled and boudinaged, progressively rotated towards parallelism with gneissic foliation, and metamorphosed to fine-grained biotite-plagioclase granofels. Dike orientations scatter widely as a result of variable initial orientation or variable degree of deformation. The most planar, least deformed dikes generally trend east-west and are steeply dipping.

Migmatitic gneisses were metamorphosed at upper amphibolite-facies to lower granulite-facies conditions [*Smith*, 1992; *Luyendyk et al.*, 1992]. Mineral assemblages associated with both S_2 and S_3 define similar temperature and pressure conditions for the two deformational/metamorphic phases. No compositional variation exists between inclusion-filled cores of M_2 garnet porphyroblasts (in S_2) and their inclusion-free M_3 overgrowths; individual M_3 garnet porphyroblasts also have similar compositions. It is unclear whether the M_2 and M_3 assemblages formed during related or distinct events, but it is clear that during M_3 the rocks fully equilibrated at temperatures above ~650°C to allow homogenization of garnet compositions [*Tracy*, 1982; *Spear*, 1988]. Garnet-biotite and garnet-cordierite thermometry record temperatures of 725°-780°C from the highest-grade rocks with S_3 fabric [*Smith*, 1992]. Pressures of 4.3-5.6 kbar are calculated for the same rocks using the garnet-aluminosilicate-quartz-plagioclase barometer [*Newton and Haselton*, 1981; *Ganguly and Saxena*, 1984; *Koziol and Newton*, 1988], corresponding to depths of 15-20 km.

High-grade metamorphic conditions persisted after deformation and S_3 development had ceased. Unit 2 anatectic melts crosscut the gneissic foliation, both on the outcrop scale and in the large block gneiss bodies. Preservation of euhedral aluminosilicate porphyroblasts is an indication that no penetrative subsolidus deformation occurred after crystallization of the anatectic melts. Postkinematic metamorphic recrystallization in the gneissic rocks has obliterated deformation-related textures. Mineral lineations in the gneiss are rare and not consistently oriented.

Cordierite rims on M_2 garnet porphyroblasts and symplectic reaction textures suggest that an initial phase of decompression occurred while high-temperature conditions were maintained. Cooling was rapid enough that retrograde compositional zoning did not develop in large garnet porphyroblasts. The geometry of late synmetamorphic extensional shear fractures and mafic dikes suggest a NNE component of extension during the late stages of the second deformation event. Extension fractures filled with muscovite-bearing retrograde pegmatites and younger quartz-epidote-muscovite veins trend ESE, indicating a NNE extension direction during cooling [*Richard*, 1992].

Geology of Ranges Adjacent to the Fosdick Mountains

Unfoliated, medium-grained, equigranular granodiorite of the Ford granodiorite underlies most of the Chester Mountains and the Mt. June area of the Phillips Mountains (Figure 3). Throughout the Chester Mountains, and to a lesser degree in the Phillips Mountains, hornblende in the Ford granodiorite is replaced by biotite. Foliated to gneissic granodiorite at Neptune Nunatak is interpreted to represent a structurally deep part of the Ford granodiorite batholith in the Chester Mountains. Small bodies of equigranular medium- to fine-grained muscovite-biotite leucogranite intrude Ford granodiorite in the Chester Mountains and the foliated granodiorite at Neptune Nunatak. These plutons have yielded U-Pb zircon ages of 240 Ma (D. L. Kimbrough, unpublished data, 1992). The Byrd Coast granite is an equigranular, unfoliated alkali-feldspar granite that underlies the eastern part of the Phillips, Fosdick, and Chester mountain blocks (Figure 3). These granites have A-type chemistry in the study area (D. L. Kimbrough, unpublished data, 1992). The granite is epizonal, based on the presence of miarolitic cavities with terminated quartz crystals and local gradation into granite porphyry upward on Mt. Carbonne. Contacts between Byrd Coast granite and Ford granodiorite or FMC are not exposed in the study area, but dikes of granite porphyry strongly resembling Byrd Coast granite intrude Ford granodiorite near their contact between Mt. June and Mt. Paige in the Phillips Mountains, consistent with Byrd

Table 1. Monazite U-Pb data from Fosdick Mountains

Sample	Size[a]	Weight, mg	Concentration Pb, ppm	Concentration U, ppm	Pb Isotopic Composition[b] 208/206	207/206 × 10^{-2}	204/206 × 10^{-3}	Radiogenic Ratios, Age, and Error 206*/238	Age, Ma	Error %	207*/235	Age, Ma	Error %	207*/206*	Age, Error Ma	%
Fosdick Mountains Paragneiss																
Marujupu 2	cg	5.6	201.1	6608	0.7851	11.71	4.767	0.01687	107.8	0.30	0.10881	104.9	0.66	0.04679	39	13
	fg	5.8	341.9	10890	1.214	5.192	0.259	0.01665	106.5	0.22	0.11048	106.4	0.22	0.04812	105	2
	bulk	6.8	328.2	10370	1.154	5.039	0.153	0.01658	106.0	0.31	0.11003	106.0	0.31	0.04814	106	2
Bird Bluff 3	fg	2.9	293.8	5904	1.958	12.51	5.273	0.01683	107.6	0.21	0.10974	105.7	0.68	0.04730	65	14
Fosdick Mountains Postkinematic Granitoid																
Avers 1	bulk a	1.7	224.4	1679	8.559	6.428	1.121	0.01570	100.4	0.23	0.10339	99.9	0.39	0.04776	87	7
	bulkb	4.4	209.0	1571	8.520	6.282	1.029	0.01571	100.5	0.21	0.10327	99.8	0.37	0.04766	82	7

Monazite was dissolved with 12 *N* HCl at 220°C with a second dissolution cycle following evaporation to dryness. Separation of U and Pb was done using HCl column chemistry. Isotopic ratios were measured with the SDSU VG Sector 54 multicollector thermal ionization mass spectrometer. $^{206}Pb/^{204}Pb$ ratios were measured using a Daly multiplier. Concentrations were determined using a mixed $^{208}Pb/^{235}U$ spike. Ages calculated using the following decay constants: ^{238}U, 1.55125×10^{-10} and ^{235}U, 9.8485×10^{-10}. Present day $^{238}U/^{235}U = 137.88$. Accuracies of the $^{206}Pb/^{238}U$ dates, which include uncertainties in the spike calibrations are estimated to be better than 0.5%. Corrections for common lead were made using *Stacey and Kramers* [1975] lead model isotopic compositions for the interpreted crystallization age. Lead blanks < 100 pg total common lead per analysis. Errors were determined using the data reduction program of *Ludwig* [1989]. **Asterisks indicate radiogenic component.**

[a] Size fractions analyzed include fg, fine grained (<200 mesh), cg, coarse grained (>200 mesh), and bulk; bulk a and bulk b from Avers 1 sample are splits from zircon concentrate.

[b] Lead isotopic compositions have been corrected for 0.125% per mass unit mass fractionation based on replicate analyses of common lead isotopic standard NBS981 from the U. S. National Bureau of Standards.

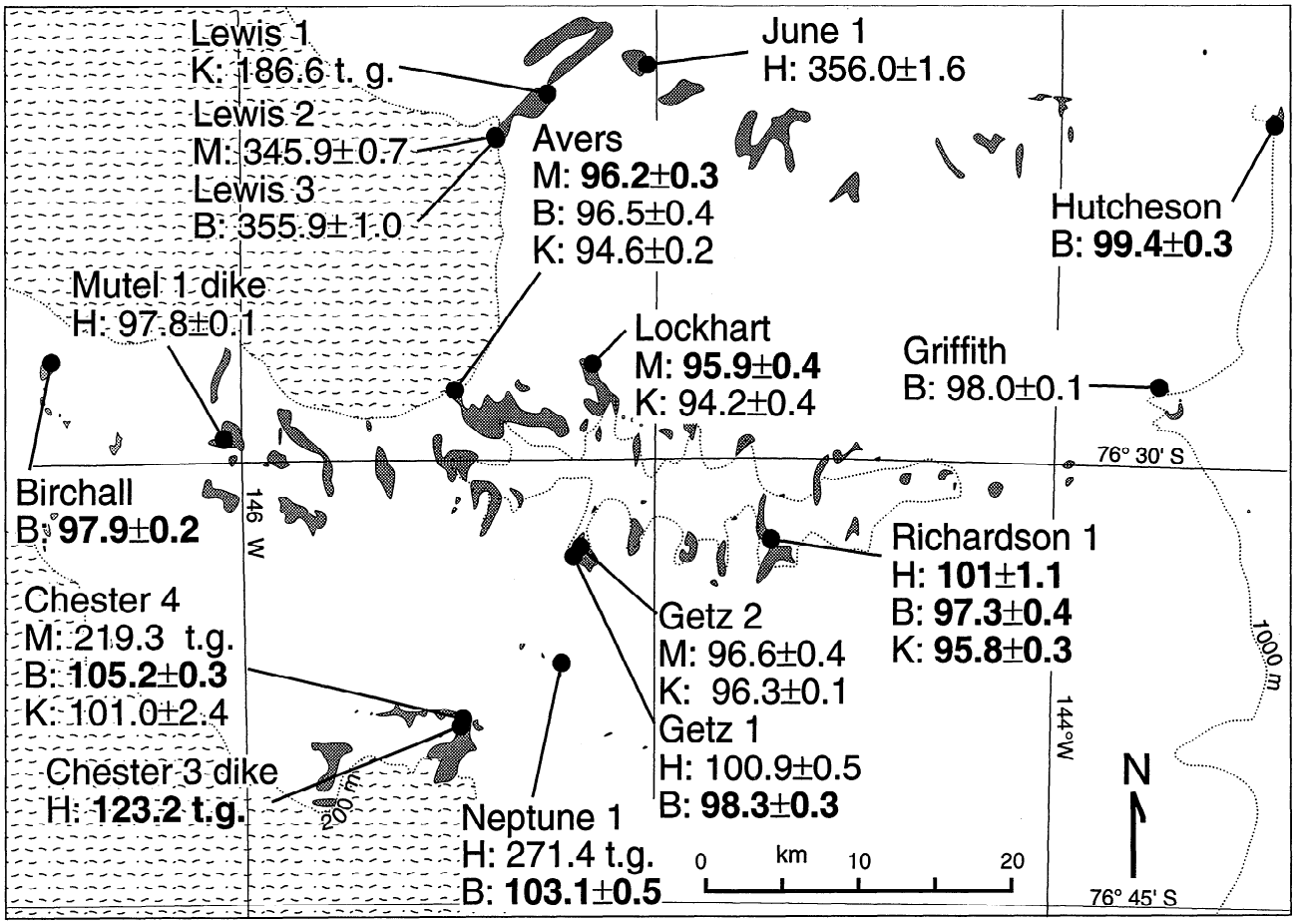

Figure 4. Map showing location of $^{40}Ar/^{39}Ar$ samples and summarizing cooling ages. Dates in bold-face type are for samples that yielded concordant plateau and isochron ages. (See Table 3 for a summary of all data.) The "t.g." indicates total gas apparent age.

Coast granite intruding Ford granodiorite. U-Pb systematics of zircon and monazite from Byrd Coast granite samples from Mt. Corey and Hutcheson Nunatak indicate an intrusive age of 103-105 Ma (D. L. Kimbrough, unpublished data, 1992).

Thermochronology

We have established a time-temperature path for rocks of the Fosdick, Chester, and Phillips mountains and adjacent ranges using U-Pb, $^{40}Ar/^{39}Ar$, and fission track thermochronometers from a variety of minerals. These data document cooling from peak metamorphic conditions of ~725°C, ~4.5-5.5 kbar starting at 105 Ma, followed by a period of rapid cooling between ~101 and 95 Ma. Cooling rates slowed significantly after ~70 Ma.

U-Pb Data

Monazite from two paragneiss samples and one crosscutting two-mica granite in the FMC was separated, and the uranium and lead isotopic composition was determined using standard techniques. Analytical data are summarized in Table 1. Two fractions from Marujupu 2 paragneiss exhibit concordant ages of 106 ± 1.2 Ma. One fraction from Marujupu 2 and one fraction from Bird Bluff 3 paragneiss exhibit reverse discordance typical of many monazites, interpreted to result from incorporation of ^{230}Th in the monazite during crystallization [*Schärer*, 1984]. In these cases, the $^{207}Pb/^{235}U$ ages of 104.9 Ma and 105.7 Ma, respectively, are considered the closest approximation to the time since closure of the U-Pb system. Recent estimates of the closure temperature for the U-Pb system in monazite range from 640° to 730°C [*Copeland et al.*, 1988; *Parrish*, 1988; *Mezger et al.*, 1991], lower than the estimated peak metamorphic temperature of 760° ± 30°C reached in the highest grade part of the FMC, from which these samples were collected. The consistent results from two widely separated samples demonstrate that cooling after high-grade metamorphism in the FMC was under way by 105 Ma. Monazite fractions from a small, undeformed two-mica granite pluton that intrudes the FMC (Avers 1) exhibit slight reverse discordance, and the concordant $^{207}Pb/^{235}U$ ages of 99.9 and 99.8 Ma are interpreted to be the crystallization age of this pluton. Deformation in the FMC had clearly ended by this time.

The $^{40}Ar/^{39}Ar$ Data

The $^{40}Ar/^{39}Ar$ sample locations are indicated in Figure 4, and samples are briefly described in the Appendix. Age spectra for hornblende, muscovite, biotite, and potassium feldspar samples that did not yield concordant plateau and isochron

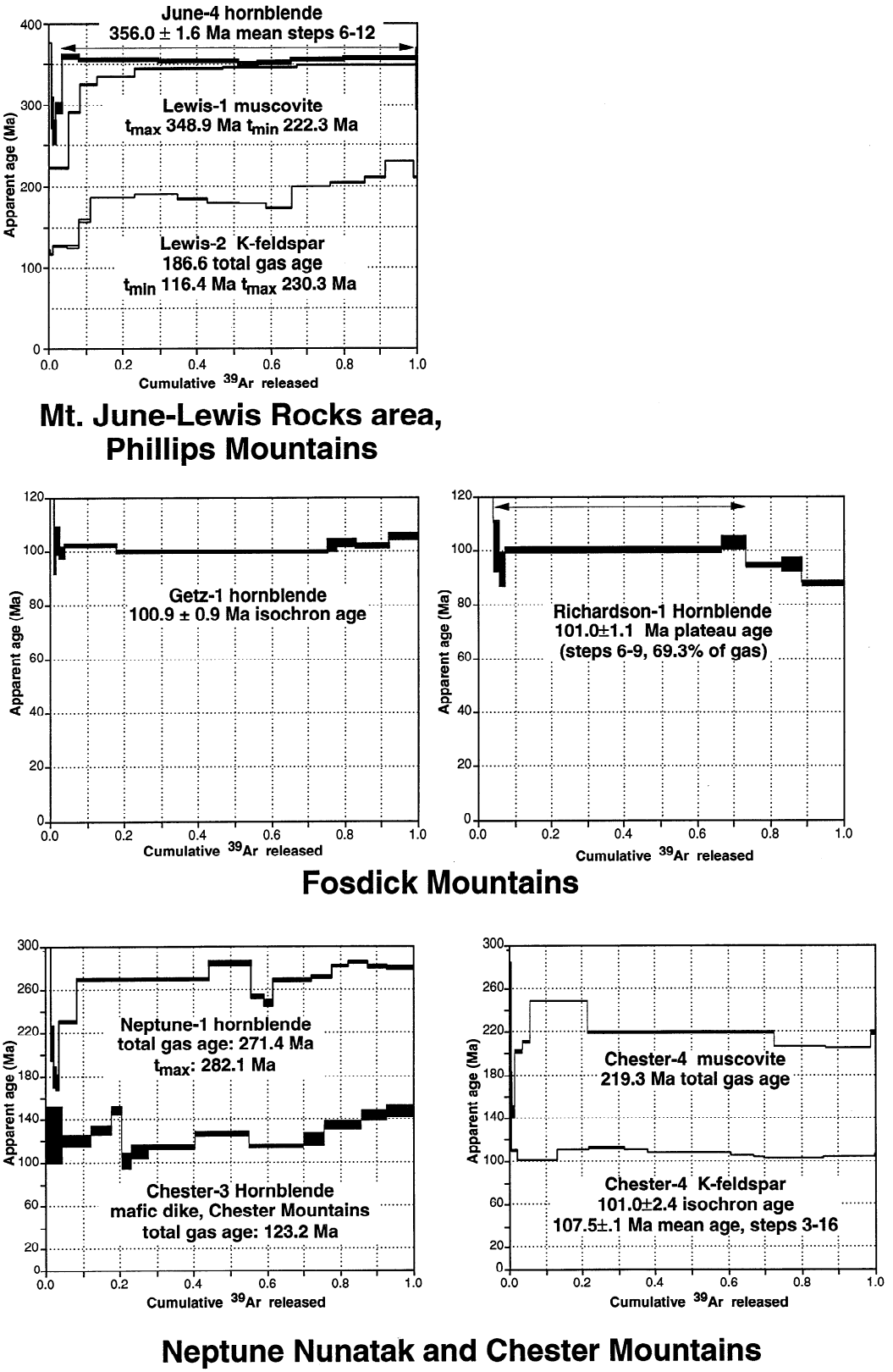

Figure 5. Age spectra for $^{40}Ar/^{39}Ar$ samples that did not yield concordant plateau and isochron ages. (See discussion of interpretation in text.)

Table 2. Closure Temperatures Used for Cooling Histories

Mineral	Closure Temperature, °C
Monazite	730
Hornblende	525
Muscovite	340
Biotite	325
K-feldspar	165
Apatite (>PAZ)	120
Apatite (<PAZ)	60

Closure temperatures for hornblende, muscovite, biotite, and K-feldspar were calculated for a cooling rate of 100°C/m.y. using the equations of *Dodson* [1973] and diffusion parameters summarized by *McDougall and Harrison* [1988]. Abbreviations: >PAZ, upper limit of partial annealing zone, <PAZ, lower limit of partial annealing zone.

ages are also presented in Figure 5. Analytical data are presented in the Supplementary Table[1], and the $^{40}Ar/^{39}Ar$ results are summarized in Table 3. A plateau is defined to include >50% of the ^{39}Ar released in at least three contiguous steps, with all ages on the plateau statistically indistinguishable at the 95% confidence level [*McDougall and Harrison*, 1988]. Closure temperatures used here are summarized in Table 2. Samples that yielded concordant plateau and isochron ages are interpreted to record a simple history of cooling (rapid cooling in the case of K-feldspars) from temperatures well above the closure temperature to below the closure temperature. Interpretation of samples that did not yield concordant plateau and isochron ages is discussed below.

Chester Mountains. Biotite, muscovite, and K-feldspar were analyzed from a small muscovite-biotite granite body intruding Ford granodiorite in the Chester Mountains (sample Chester 4). The body is lithologically identical to a similar body in the Neptune Nunataks that has yielded a U-Pb age from zircon of 240 Ma (D. L. Kimbrough, unpublished data, 1992). Muscovite from this sample yielded a slightly disturbed spectra; no simple explanation can be proposed for the anomalously old step 5. The average ages for steps 6-8, accounting for 77% of the ^{39}Ar released, is 207.7 ± 0.3 Ma. K-feldspar yielded a slightly disturbed spectra with a minimum apparent age of 101.7 Ma and a total gas age of 108.4 Ma. The isochron age for this sample, based on steps 6-16, for which radiogenic yields are >95%, is 101.0 ± 2.4 Ma, with an initial $^{40}Ar/^{36}Ar$ ratio of ~904. The old apparent ages of steps 1 and 2 indicate significant inherited radiogenic argon in low-temperature sites; the high initial ratio suggests that radiogenic argon degassed from the surrounding Paleozoic igneous rocks during a Cretaceous thermal event has permeated K-feldspar in this sample.

Neptune Nunataks. Biotite and hornblende were analyzed from foliated granodiorite on Neptune Nunatak which is lithologically similar to Ford granodiorite of the Chester Mountains. Microprobe analyses of hornblende from this sample indicate the presence of three intergrown amphibole phases. The complex spectra from the Neptune 1 hornblende is consistent with the mixing of amphibole phases observed in the sample [cf. *Harrison and FitzGerald*, 1986]. Total gas age for this hornblende is 271.4 Ma, and the maximum age is 282 Ma (average of the four highest temperature steps). Hornblende from this sample is interpreted to have originally closed to Ar diffusion soon after emplacement at ~350 Ma, assuming a cooling history similar to Ford granodiorite samples from the Phillips Mountains (see below) and other parts of the Ford Ranges [*Adams*, 1987]. Some Ar loss may have occurred in association with the intrusion of unfoliated Permian two-mica granite that crops out on the central Neptune Nunatak. The minimum apparent age of 174 Ma suggests additional Ar loss during a thermal event associated with intrusion of Byrd Coast granite and metamorphism in the FMC at ~100 Ma. The biotite cooling age from this sample (Table 3) records cooling after the Cretaceous metamorphic event.

Fosdick Mountains. Cooling ages from the FMC in the central Fosdick Mountains range from 101 Ma from hornblende to 94.2 Ma from K-feldspar. Many of the minerals analyzed were extremely well behaved and yielded concordant plateau and isochron ages (Table 3). Hornblende from Mt. Richardson (Richardson 1) yielded a slightly disturbed age spectrum. Steps 6-9 have statistically indistinguishable apparent ages (due in part to large errors on steps 6 and 7) and yield a plateau age of 101.0 ± 1.1 Ma. The isochron age for these four steps is 104.1 ± 0.7 Ma, with an initial $^{40}Ar/^{36}Ar$ ratio of 278 ± 9. The difference between these dates is statistically significant [*Dalrymple and Lanphere*, 1969]. Because biotite and K-feldspar from Richardson 1 both yielded excellent isochrons with atmospheric initial ratios (Table 3), the low initial ratio calculated from the regression is considered spurious, and the plateau (mean) age is used to represent the time of final closure for this hornblende. Hornblende from Mt. Getz (sample Getz 1) yielded a slightly saddle-shaped spectrum with an isochron age of 100.9 ± 0.9 Ma (initial $^{40}Ar/^{36}Ar$ ratio = 309). Biotite from the Avers sample was analyzed by laser fusion of groups of two to four grains. Results from six analyses are statistically indistinguishable and have a mean apparent age of 96.5 ± 0.4 Ma.

Phillips Mountains. Hornblende from the eastern part of the Ford granodiorite pluton in the Mt. June area of the Phillips Mountains (sample Lewis 1) yielded a slightly disturbed age spectrum; the mean age of steps 5-12 (96.6% of ^{39}Ar released) is 356.0 ± 1.6 Ma, which is not significantly different from the isochron age of 350.6 ± 2.5. Sample Lewis 1 was collected ~10 km north of sample Lewis 3, which yielded an identical or slightly older biotite cooling age (Table 3). Both the hornblende and biotite cooling ages are close to the probable crystallization age of this pluton, ~360 Ma, based on lithologic correlation with dated Ford granodiorite in the Chester Mountains (D. L. Kimbrough, unpublished data, 1991). The concordance of the biotite and hornblende cooling ages probably reflects rapid cooling instead of slightly different cooling history from north to south across Mt. June. K-feldspar from an aplite dike in the Ford granodiorite (sample Lewis 1) yielded a complex age spectra suggestive of mixed

[1]Supplementary Table is available with entire article on microfiche. Order from American Geophysical Union, 2000 Florida Ave., N.W., Washington, D. C. 20009. Document T93-005; $2.50. Payment must accompany order.

Table 3. Summary of $^{40}Ar/^{39}Ar$ Results

Sample	Mineral	Mean Age[a]		Steps	Percent of Gas	Isochron	Age[b]	Steps	Initial Ratio	
Avers	biotite	96.5	±0.4[c]							
Avers	K feldspar	(94.6)	(±0.2)	2 17	99.8	(94.3)	(±0.6)	2 17	288	±18
Avers	muscovite	(96.2)	(±0.3)	all	100.0	(96.4)	(±0.1)	all	293	±6
Birchall	biotite	(97.9)	(±0.2)	8 14	61.7	(97.8)	(±0.2)	1 10,12	388	±39
Chester 3	hornblende	123.2[d]								
Chester 4	biotite	(105.2)	(±0.3)	4 7	63.3	(105.0)	(±0.3)	all	305	±17
Chester 4	K-feldspar	107.5	±0.1	3 14	99.5	(101.0)	(±2.4)	6 16	904	±262
Chester 4	muscovite	219.3[d]								
Getz 1	biotite	(98.3)	(±0.3)	4 9	77.5	98.2	±0.3	all	323	±46
Getz 1	hornblende	100.9	±0.5	7 11	87.0	100.9	±0.9	all	309	±8
Getz 2	K feldspar	96.3	±0.1	4 13	93.7	(97.0)	(±0.2)	2 13	263	±29
Getz 2	muscovite	(96.6)	(±0.4)	1 11	95.7	(97.0)	(±0.4)	9 14	294	±2
Griffith	biotite	98.0	±0.1	3 16	93.2	(97.7)	(±0.1)		406	±38
Hutcheson	biotite	(99.4)	(±0.3)	5 7	54.7	(99.3)	(±1.0)	2 7	338	±76
June 1	hornblende	356.0	±1.6	5 12	96.6	(350.6)	(±2.5)	6 12	390	±50
Lewis 1	K-feldspar[e]	186.6[d]								
Lewis 2	muscovite[f]	345.9	±0.7	5 11	77.0					
Lewis 3	biotite	(355.9)	(±1.0)	8 15	50.8	(356.0)	(±1.0)	2 15	272	±47
Lockhart 1	K-feldspar	(94.2)	(±0.4)	3 14	98.1	(95.2)	(±0.7)	3 14	276	±18
Lockhart 1	muscovite	(95.9)	(±0.4)	all	100.0	(96.1)	(±0.2)	all	288	±9
Mutel 1	hornblende	(97.8)	(±0.1)	6 11	89.5	(96.4)	(±1.1)	6 11	330	±22
Neptune 1	biotite	(103.1)	(±0.5)	2 6	96.0	(104.0)	(±1.1)	2 6	275	±18
Neptune 1	hornblende[g]	271.4[d]								
Richardson 1	biotite	(97.3)	(±0.4)	all	100.0	(97.4)	(±0.0)	2 7	294	±2
Richardson 1	hornblende	(101.0)	(±1.1)	6 9	69.3					
Richardson 1	K feldspar	(95.8)	(±0.3)	2 17	99.9	(95.2)	(±0.4)	2 17	306	±10

[a]Plateau ages reported in parentheses

[b]Isochron ages reported in parentheses are concordant with plateau age (corresponding mean age also in parentheses) or are the interpreted cooling age used (corresponding mean age without parentheses).

[c]Mean of six laser fusion experiments

[d]Total gas date

[e]t_{max} = 230.3 Ma; t_{min} = 116.4 Ma

[f]t_{max} = 348.9 Ma; t_{min} = 222.3 Ma

[g]t_{max} = 282.1 Ma, mean of steps 14-17

diffusion domain sizes within the sample [*Zeitler*, 1987; *Lovera et al.*, 1989]. Apparent ages of most of the step heating increments from this sample are between 170 and 230 Ma. Younger ages between 116 and 126 Ma from the lowest-temperature steps are consistent with some Ar loss associated with intrusion of Byrd Coast granite and metamorphism in the Fosdick Mountains. This feldspar is interpreted to record a combination of slow postcrystallization cooling and later diffusional Ar loss. White mica from a quartz-sericite vein in Ford granodiorite (sample Lewis 2) was collected to test the possibility that scattered quartz veins in the Ford granodiorite were associated with Byrd Coast granite intrusion and metamorphism in the FMC. The plateau age of 348 Ma from this muscovite is younger than biotite from Ford granodiorite collected ~100 m from the quartz vein (sample Lewis 3), suggesting that the introduction of the quartz veins occurred at temperatures below the biotite closure temperature and did not significantly heat the surrounding rock. The plateau age is interpreted to approximate the time of formation of the quartz veins, soon after crystallization of the Ford granodiorite. Progression to younger apparent ages from lower-temperature steps suggests minor argon loss sometime after 220 Ma. Together, these data indicate that the Ford granodiorite in the Mt. June area had cooled below closure temperatures for biotite soon after its crystallization and was below the Ar closure temperature for K-feldspar before peak metamorphic conditions were achieved in the FMC.

Hutcheson Nunatak. The 99.4 ± 0.3 Ma biotite cooling age from Byrd Coast granite at Hutcheson Nunatak indicates rapid cooling after intrusion of the granite at ~103 Ma (U-Pb, monazite) (D. L. Kimbrough, unpublished data, 1992), consistent with textural evidence that the Byrd Coast granite plutons in this area are epizonal.

Mafic dikes. Hornblende from a mafic dike intruding the Ford granodiorite in the Chester Mountains (Chester 2) is complexly zoned with light greenish, actinolitic rims and dark green cores. A hand-picked concentrate of dark hornblende was analyzed and yielded a complex age spectra with apparent ages varying irregularly between 102 and 148 Ma; total gas age of this sample is 122 Ma. This spectrum is interpreted to

Table 4. Fission Track Analytical Results, Fosdick Mountains

Sample	Number of Grains	Track Density, $\times 10^6 cm^2$ Standard	Fossil	Induced	Correlation Coefficient	χ^2 Probability	Age, Ma	U, ppm	Mean Track Length, μm	Standard Deviation, μm
Avers 1	13	1.5 (9567)	0.746 (488)	2.373 (1553)	0.943	3	75 ± 4 73 ± 7[a]	16	13.9 ± 0.2 (68)	1.4
Chester 1	21	1.48 (9547)	0.602 (384)	1.505 (960)	0.847	35	95 ± 6	10	13.5 ± 0.2 (95)	1.6
Lockhart 1	10	1.49 (7124)	0.411 (164)	1.256 (501)	0.943	1.8	78 ± 7 86 ± 19[a]	8	13.9 ± 0.3 (27)	1.6
Corey 1	20	1.48 (7124)	0.517 (476)	1.548 (1426)	0.956	74	79 ± 4	10	14.6 ± 0.1 (109)	1.2
Marujupu 1	19	1.51 (9567)	0.631 (658)	1.965 (1917)	0.908	3	78 ± 4 83 ± 6[a]	13	14.4 ± 0.1 (101)	1.1
Richardson 2	11	1.47 (7124)	0.962 (231)	3.406 (818)	0.772	38	67 ± 5	23	14.0 ± 0.2 (100)	1.6

Parentheses show number of tracks counted (age data) or measured (lengths). Standard and induced track densities were measured on muscovite external detectors ($g = 0.5$) and fossil track densities on internal mineral surfaces. Ages were calculated using ζ=322 ± 4.2 for standard dosimeter glass SRM612 from the U. S. National Bureau of Standards [*Hurford and Green*, 1983]. Apatite ages were determined using the external detector method and an Autoscan™ stage. Samples were irradiated in the graphite reflector region of the V 43 position (Cd for Au ratio of ~280) at the Georgia Institute of Technology Nuclear Reactor [*Crowley*, 1986]. Thermal neutron fluences were monitored using U. S. National Bureau of Sandards reference glass SRM612. Mounts were counted at a magnification of 1250X, under a dry 100X objective. Whenever possible, 20 grains were counted. Ages were calculated using the zeta calibration method following the procedures of *Hurford and Green* [1983] and *Green* [1986]. Errors were calculated using the "conventional method" [*Green*, 1981]. Track lengths were measured in apatites on horizontal, "confined" fission tracks [*Laslett et al.*, 1984] under a 100X dry objective using a projection tube and a digitizing tablet.

[a]Mean age is used where pooled data fail χ^2.

indicate that the dikes are Early Cretaceous in age. Hornblende from an undeformed mafic dike intruding the FMC in the western Fosdick Mountains yielded concordant plateau and isochron ages of 97.8 ± 0.1 Ma and 96.4 ± 1.1 Ma, respectively.

Fission Track Data

Apatite separates were obtained from six samples used for U-Pb analysis. In general, the quality of apatite separates from the Fosdick Mountains was not high. Abundant inclusions and defects within apatite grains (e.g., Chester 1 sample) made track identification difficult for a number of the samples. Analytical data are summarized in Table 4, samples are described in the appendix, and sample locations are shown in Figure 6. Poor quality apatite and a bimodal uranium distribution within the population of apatite grains from the Lockhart 1 sample resulted in an apparent apatite age with an exceptionally large error.

Fission track ages fail the χ^2 test when non-Poissonian variability exists in the population of single-grain ages at the 95% confidence level [*Galbraith*, 1981]. Failure of the χ^2 test is usually a result of partial annealing on grains of slightly differing chemical composition (fission tracks in grains that are Cl-rich are more resistant to annealing than tracks in F-rich grains [*Green et al.*, 1986]). In samples with poor quality apatite, failure of the χ^2 test can also be due to a wide variation in apparent single-grain ages induced by poor counting statistics (e.g., Lockhart 1 sample). Ages are quoted at the 1-sigma level throughout this discussion.

All apatite ages are significantly younger than minimum $^{40}Ar/^{39}Ar$ dates from K-feldspar in nearby samples (Figures 4 and 6). Dates range from 95 ± 6 Ma at Chester 1 to 67 ± 5 Ma at Richardson. Track length distributions reflect rapid cooling with means of ~14 μm and standard deviations of <1.6 μm (Table 4 and Figure 6). Compared with the K-feldspar $^{40}Ar/^{39}Ar$ dates, the younger fission track dates indicate a slowing of the rate of cooling after ~95 Ma. Forward modeling [*Laslett et al.*, 1987; *Green et al.*, 1989], in conjunction with the data from the other thermochronologic techniques, was used to constrain low-temperature cooling histories consistent with measured track length distributions and ages. The age of the Chester 1 sample (95 ± 6 Ma) is concordant within error with K-feldspar plateau ages from the FMC, indicative of rapid cooling almost entirely through the apatite partial annealing zone (~110°-60°C) by 90 Ma, although the mean track length of 13.5 μm and standard deviation of 1.6 μm indicate that some annealing has occurred. Long mean track length and low standard deviation of the distribution from Marujupu 3 indicate rapid cooling through the partial annealing zone at ~80 Ma, suggesting cooling rates of the order of 50°C/m.y. Data from the two samples closest to Marujupu 3, Lockhart 1 and Avers 1, although poor, are consistent with similar rapid cooling between ~75 and ~80 Ma. The slightly larger standard deviations of the Richardson and Chester 1 data are consistent

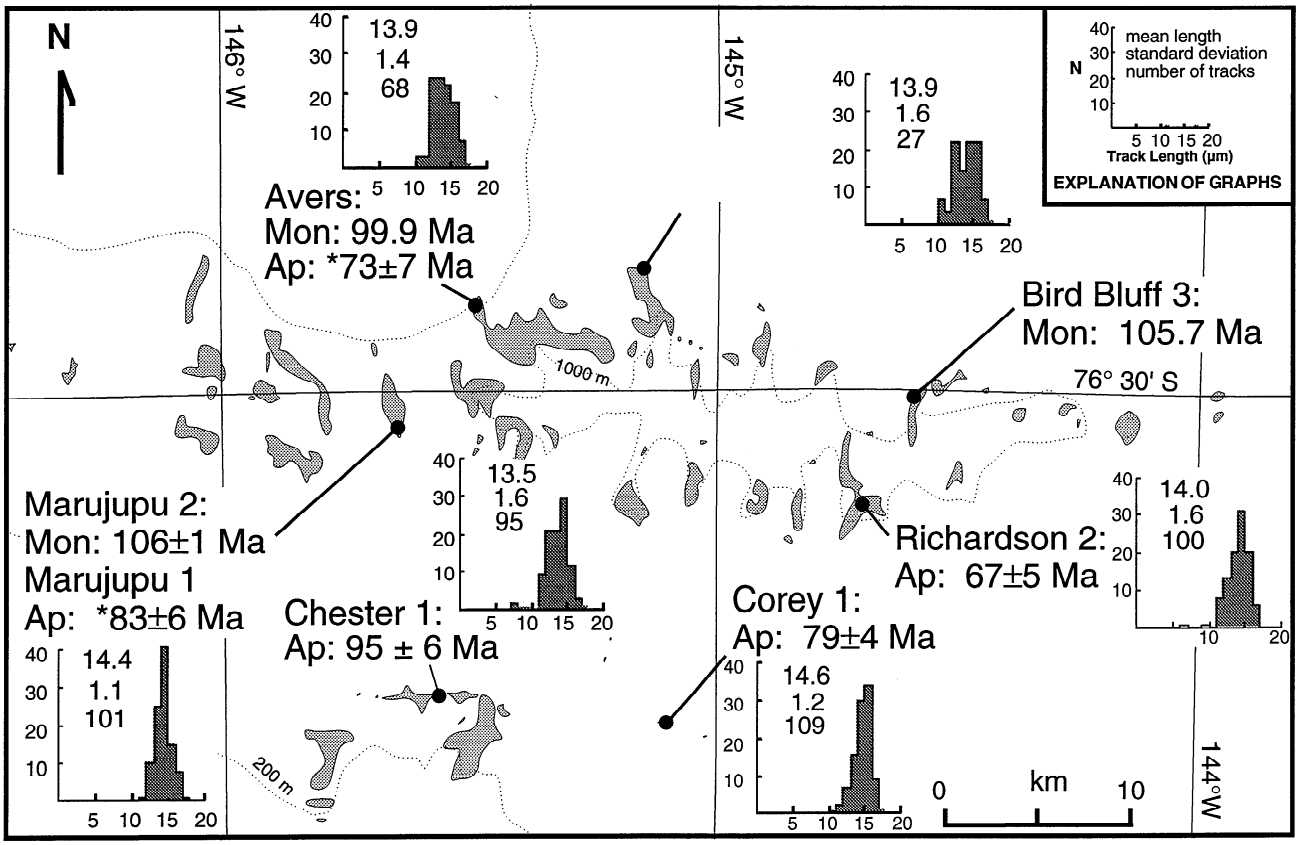

Figure 6. Fission track cooling ages and track length distributions and monazite U-Pb ages for samples from the Fosdick Mountains area. Asterisks indicate fission track dates that failed the χ^2 test (see text).

with slower cooling rates. Except for the Richardson sample (67 ± 5 Ma), in all models the cooling rate slows to ~1°C/m.y. after ~70 Ma for the duration of the cooling history. The fission track data from Byrd Coast granite (sample Corey 1) are consistent with the cooling pattern from samples in the FMC (rates of >50°C/m.y. until ~80 Ma, then slower cooling at rates of ~1°C/m.y.), suggesting that rocks in all sample localities reached shallow crustal levels at about the same time. Two explanations are possible for the relatively young age of 67 ± 5 Ma from the Richardson 2 sample. In the first model the sample resided at temperatures between ~165°C (closure temperature for K-spar) and ~110°C until ~75 Ma, then cooled at ~10°C/m.y. through the partial annealing zone, followed by slower cooling. The second model is based on the observation that Quaternary (W. C. McIntosh, written communication, 1991) basaltic lavas blanket the eastern Fosdick Mountains, and remnants of these basalts are preserved on the east and south side of Mt. Richardson (Figure 3). The Richardson sample site may have been heated by lava flows. However, to reduce the age of the Richardson sample by ~10 Ma (relative to the other samples) because of partial annealing during the Quaternary would shift the mode of the track length distribution significantly toward shorter lengths. Such a trend is not seen. It is possible then that the younger age of Richardson in the east reflects later cooling or greater denudation as deeper crustal levels are exhumed.

Summary of Cooling History

Figure 7 presents cooling paths interpreted from the combined thermochronologic data set. Byrd Coast granite intrusion occurred between 100 and 105 Ma, and these plutons cooled very rapidly (>100°C/m.y.) to below biotite closure temperature, consistent with their epizonal character. Ford granodiorite in the Phillips Mountains was below K-feldspar closure temperatures by early Cretaceous time but might have experienced a short-lived thermal pulse to produce some argon loss from K-feldspar during the intrusion of Byrd Coast granite and metamorphism in the Fosdick Mountains. The Chester Mountains were below muscovite closure temperatures by Jurassic time. On the basis of the lithologic similarity of Ford granodiorite in the Chester and Phillips mountains we infer that the early cooling history in the two ranges was similar, in which case the Chester Mountains would have cooled below K-feldspar closure temperatures before a Cretaceous reheating event. Subsequent rapid cooling at ~70°C/m.y. yielded biotite and K-feldspar cooling ages of 105 and 101 Ma respectively. Apatite fission track data are interpreted to indicate continued rapid cooling until ~95 Ma, when the rate decreased dramatically to ~1°C/m.y.. Monazite U-Pb data from high-grade metapelites in the FMC are interpreted to indicate that temperatures of >700°C persisted until ~104 Ma. Metamorphic rocks in the FMC then cooled rapidly to K-feldspar closure tempera-

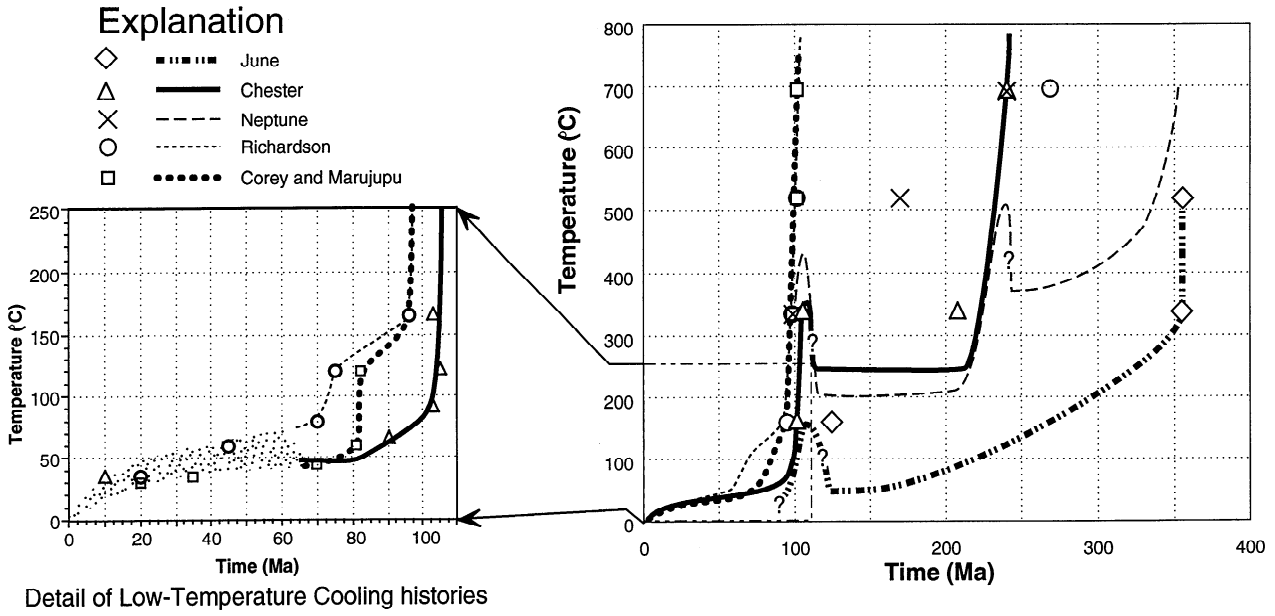

Figure 7. Cooling paths for rocks in the Fosdick Mountains region based on thermochronologic data. Detail of low-temperature history is provided for Chester, Richardson, and central FMC (based on Marujupu and Corey) (left). Cooling history is based on forward modeling of fission track length distributions. Complete cooling paths are given for rocks in the western Phillips Mountains, Fosdick Mountains, Neptune Nunataks and Chester Mountains (right). The Byrd Coast granite path is a composite from Hutcheson and Corey data.

ture (~165°C) by 94 Ma. The average cooling rate calculated for this interval is 70° ± 30°C/m.y. The discrepancy between the K-feldspar $^{40}Ar/^{39}Ar$ and apatite fission track cooling ages indicates that the cooling rate slowed between ~94 and 80 Ma, with an average rate of 4° ± 1°C/m.y. Fission track cooling ages and track distributions are consistent with cooling from 120°C to 60°C at rates as high as 50°C/m.y., starting at ~80 Ma. Cooling rates decreased to ~1°C/m.y. by ~70 Ma, and slow cooling continued for the duration of the cooling history.

Heating associated with Fosdick metamorphism was intense enough to reset biotite and K-feldspar in the Chester Mountains but not hornblende at Neptune Nunatak or muscovite in the Chester Mountains. Cooling ages for each mineral system progress from older to younger from the Chester Mountains to the northern Fosdick Mountains (Figure 8). On the basis of their pre-Cretaceous cooling ages, rocks from the Mt. June area in the Phillips Mountains are interpreted to have resided at a higher structural level than the Chester Mountains, such that none of the $^{40}Ar/^{39}Ar$ mineral systems was reset during the Cretaceous metamorphic event.

Thermal Modeling

Rapid cooling requires high thermal gradients. When high-grade metamorphic rocks cool rapidly, such gradients can be produced by large normal faults during regional extension or may result from a large heat flux in the crust by intrusion or increased temperature at the base of the crust. In order to determine the conditions necessary to explain the observed cooling rates, we modeled the thermal evolution for a variety of tectonic scenarios using a one-dimensional finite difference computer program [*Peacock*, 1989, 1990]. Parameters varied were volume and temperature of intrusion into the crust, heat flux from the mantle, and exhumation rate.

We found that the observed time-temperature history could be modeled well if the geothermal gradient is elevated by the emplacement of a 2-km-thick, midcrustal sill and a 10-km-thick, lower crustal sill at the onset of metamorphism and if postmetamorphic cooling was accompanied by exhumation at 1.5 mm/yr. The upper 2-km-thick sill represents the synmetamorphic igneous complex (unit 2), which makes up as much as 75% of present exposures of the FMC, as a single granodioritic sill intruded at a temperature of 900°C. The depth and thickness of this sill are based on geobarometric results for metapelites underlying the sill complex (4.5-5.5 kbar, corresponding to 15-20 km) and on the exposed structural thickness of unit 2 rocks in the FMC. A high-temperature (1100°C) basaltic sill is incorporated into the model between depths of 25 and 35 km. The thermal effect of such an intrusion is equivalent to a dramatic increase in mantle heat flux, and this sill should be thought of as representing a combination of magmatic underplating and increased heat flux at the base of the crust [cf. *Zen*, 1992]. Other physical properties and initial conditions for the model are summarized in Table 5.

Figure 9a shows the time-temperature path based on the computer model compared with the path determined from available thermochronologic data. The path calculated represents rocks that start at a depth of 18 km, corresponding to the northern Fosdick Mountains, below most of the exposed Cretaceous synmetamorphic sill complex and within the zone of high-grade metamorphism. Igneous sills are emplaced at 105 Ma in the model, and heat from these intrusions increases the geothermal gradient for a 15-m.y. period (see Figure 9b). Initially, the geothermal gradient increases rapidly enough that

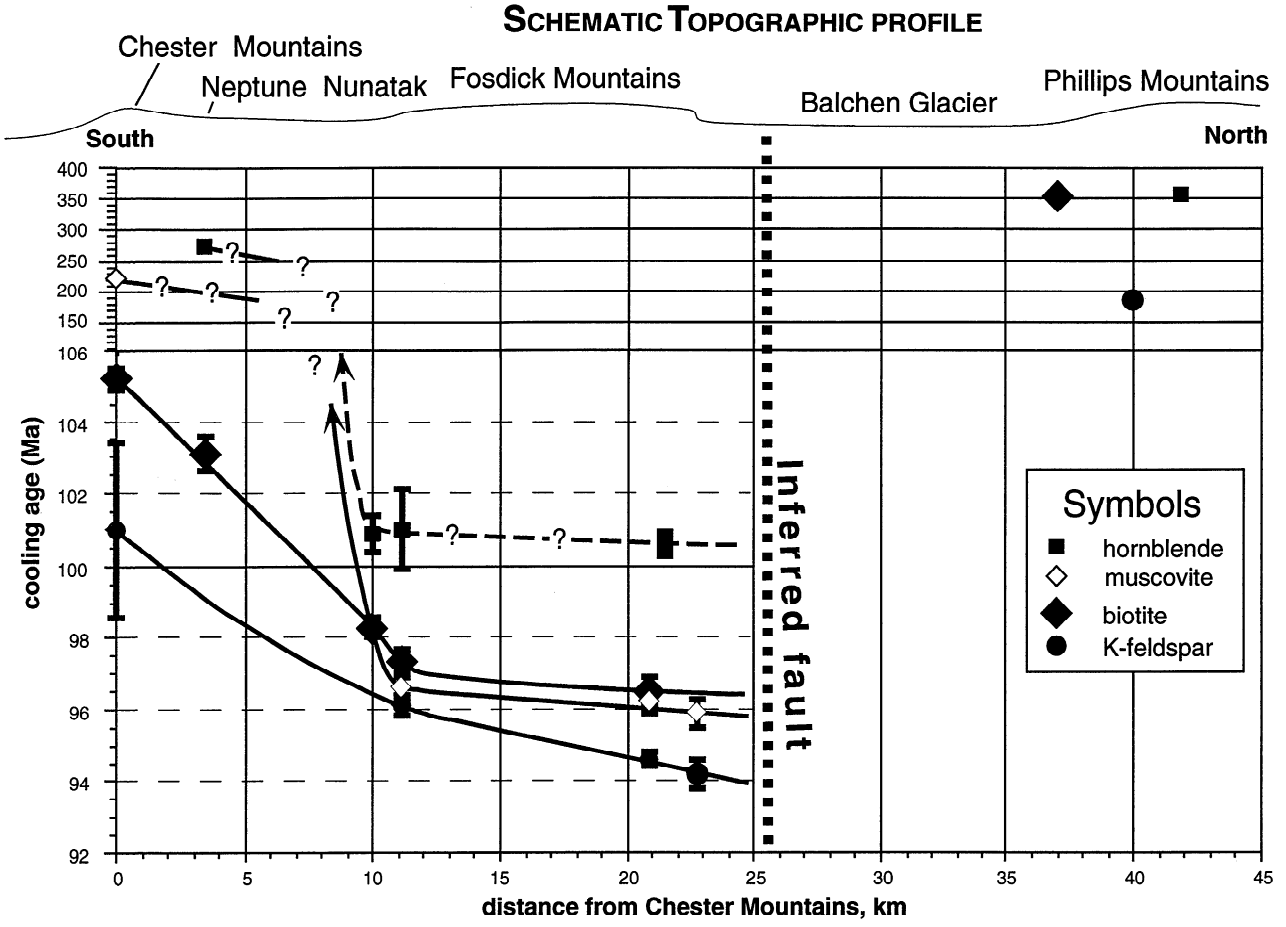

Figure 8. North-south section showing progression in cooling ages from south to north from the Chester Mountains to the Phillips Mountains. Data from the Chester, Neptune, Getz, Richardson, Lockhart, Avers, Lewis Rocks, and Mt. June samples have been projected into the line.

exhumation results in isothermal decompression. This is followed by a period during which the geothermal gradient does not change as rapidly but is near its maximum and rapid cooling begins. After some 20 m.y. of thermal evolution the geothermal gradient begins to decrease toward its initial condition, assuming that the mantle heat flux returns to a normal value and that heat production in magmatic additions to the crust is similar to that in the preexisting crust. The decreasing geothermal gradient results in decreasing cooling rate.

The model is consistent with the initial phase of isothermal decompression indicated by petrographic relationships, subsequent rapid cooling shown by $^{40}Ar/^{39}Ar$ thermochronometry, and the decreasing rate of cooling at low temperatures after closure of the K-feldspar $^{40}Ar/^{39}Ar$ system. The observed high-temperature, low-pressure metamorphism and rapid cooling rates in the FMC can be explained by conductive cooling of continental crust in which the geothermal gradient has been increased by magmatic advection in combination with exhumation at 1.5 mm/yr.

Interpretation

Intrusion of Byrd Coast Granite

Byrd Coast granite from Mt. Corey and Hutcheson Nunatak has a cooling history that is identical to that from the FMC within the resolution of the data available. Although contacts between Byrd Coast granite and other rocks are not exposed in the study area, the presence of Byrd Coast granite throughout the eastern part of the study area, dikes of the granite in Ford granodiorite in the Phillips Mountains, and regional relationships [*Wade et al.*, 1977a, b, 1978; *Weaver et al.*, 1991] all suggest that the contacts are intrusive. The very high cooling rates at Hutcheson Nunatak are consistent with intrusion into cool rocks at shallow crustal levels. No cooling data are available from Byrd Coast granite at O'Connor Nunatak (Figure 3), but the similar character of the rocks suggests a similar cooling history to Hutcheson and Corey. If Byrd Coast granite intruded the Fosdick-Chester block (as opposed to being in fault contact), then intrusion must have followed ductile deformation in the FMC and must have occurred early in the cooling history.

Faulting and Tilting in the Northern Ford Ranges

Several lines of evidence suggest that the Fosdick and Chester mountains are part of a southward tilted block. Biotite cooling ages from the Birchall, Getz 1 and Griffith samples are statistically indistinguishable, with an average age of 98.1 Ma. The very slight variation in biotite cooling ages from east to west, in conjunction with the consistent metamorphic grade in metapelitic rocks along the north side of the Fosdick

Table 5a. Physical Properties of Intrusions Used in Thermal Model

Property	Granodiorite Sill	Basaltic Sill
$T_{country\ rock}$ T_r, °C	300	450
$T_{intrusion}$ T_i, °C	900	1100
Density, kg/m^3	2750	3000
Conductivity, W/m K	2.25	1.5
Heat of crystallization, J/kg	275,000	400,000
Heat capacity, J/kg K	1000	1000
Thickness of intrusion, km	2	10

See Figure 9 for additional information. Heat capacity, temperature interval of crystallization, surface temperature, radiogenic heat production and depth scale for exponential decrease of radioactivity, and density are typical for crustal rocks. In all models, radiogenic heat production is limited to the upper 15 km of the crust [*Peacock*, 1990; *England and Thompson*, 1984]. Computer programs for one-dimensional modeling of contact and regional metamorphism were written by *Peacock* [1990]. Heat for metamorphism in the models is transferred by conduction and incorporates heat flow from the mantle into the crust or from intrusive rocks into country rocks. Internal heat is generated by radiogenic heat production. The instantaneous emplacement of sills in the middle crust and deep crust was modeled by modifying the initial geothermal gradient profile.

Mountains [*Smith*, 1992], demonstrate that there has been no significant differential uplift along the long axis of the range. In contrast, cooling ages for each mineral system progress from older to younger from the Chester Mountains to the northern Fosdick Mountains (Figure 8). The east-west trending, steeply dipping orientation of late metamorphic to post-metamorphic dikes and veins in the FMC [*Richard*, 1992] and magnetic susceptibility anisotropy data [*Luyendyk et al.*, 1992] indicate a N-S extension direction during and following the peak metamorphism. Finally, paleomagnetic data from these ranges can be interpreted to show that the Chester Mountains and the southern Fosdick Mountains have been tilted southward by 20°-30° [*Luyendyk*, 1993].

Table 5b. Boundary Conditions and Physical Properties of Crustal Rocks Used in Thermal Model

Property or Boundary Condition	Assigned Value
Mantle heat flux, mW/m	30-40
Surface temperature, °C	0
Radiogenic heat production, μW/m^3 (upper 15 km)	2.333
Conductivity, W/m K	2.25
Thermal diffusivity, x 10^{-7} m^2/s	6 to 9
Exhumation rate, mm/yr	1.5
Heat capacity, J/kg K	1000
Crustal rock density, kg/m^3	2750

See footnote for Table 5a.

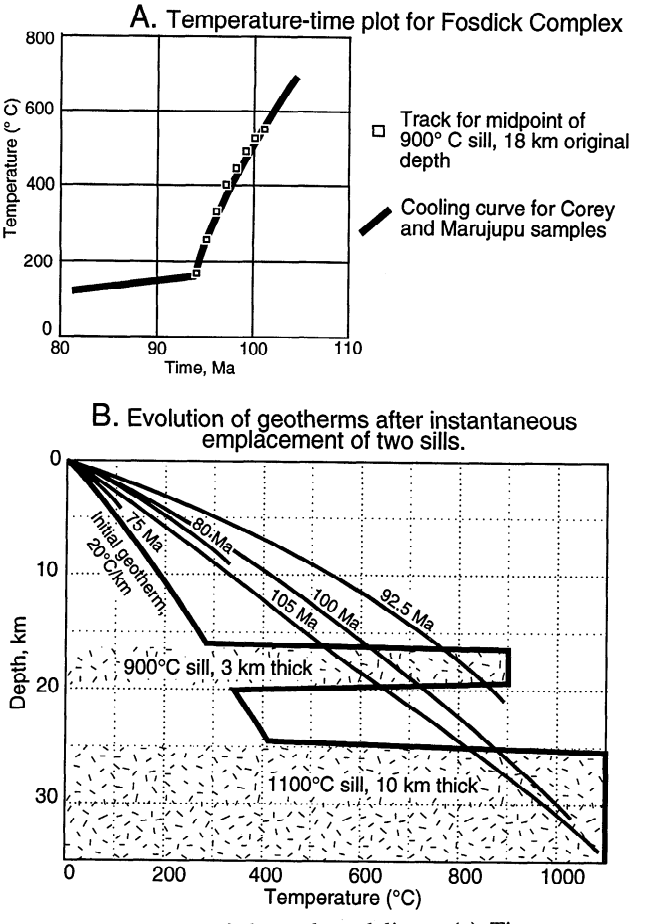

Figure 9. Results of thermal modeling. (a) Time-temperature paths are for rocks starting at 18-km-depth, corresponding to rocks presently exposed in the Lockhart-Avers area of the Fosdick Mountains. The time-temperature history for the central Fosdick Mountains based on thermochronologic data is shown for comparison. (b) Evolution of geothermal gradient in thermal model is shown for Fosdick Mountains.

Cooling ages from the Ford granodiorite in the Phillips Mountains are significantly older than those from the Chester Mountains. We interpret these results to indicate that the Mt. June area represents a significantly higher structural level in the early Cretaceous crust than either the Chester or Fosdick mountains.

The evidence for southward tilting of the Fosdick-Chester block and the higher structural level of the Ford granodiorite at Mt. June suggest that a north dipping normal fault bounds the northern Fosdick Mountains beneath the Balchen Glacier. If this fault formed during the period of rapid cooling, younging of cooling ages from south to north in the footwall of this fault (Figure 8) reflects progressive cooling as the footwall was tilted and tectonically exhumed. Alternatively, the fault may be younger, in which case the cooling age gradients reflect tilting of originally subhorizontal surfaces of equal cooling age that resulted from conductive cooling. Late stage to retrograde muscovite (plateau age of 95.9 ± 0.4 Ma) in the Lockhart 1 sample (see Appendix) is probably coeval with the late stage pegmatites in the Fosdick complex that fill east trending extension fractures. It seems likely that faulting was

coeval with or occurred soon after the development of the late metamorphic and postmetamorphic structures, starting as early as ~96 Ma.

Deformation Associated With Exhumation

We hypothesize a three-stage deformation history related to exhumation of the FMC. The earliest deformation was associated with high-grade metamorphism (D_3-M_3). Our data do not directly constrain the kinematics of D_3 deformation. The similar orientation of the least deformed, late metamorphic mafic dikes and postmetamorphic pegmatites and quartz-muscovite veins suggests a dynamic link between D_3 deformation and subsequent brittle structures associated with north-south extension. Superposition of brittle dikes and veins directly on high-grade fabrics and the absence of greenschist-facies or lower amphibolite-facies mylonite zones indicate that rocks of the FMC were not being deformed penetratively during cooling through subgreenschist-facies conditions.

The second phase of deformation is associated with rapid cooling of the FMC and commenced at ~105 Ma with the the closure of monazite U-Pb system in high-grade metapelites. Disequilibrium metamorphic textures indicative of isothermal decompression [*Smith,* 1992] are consistent with thermal models that predict a short period of isothermal decompression if the exhumation rate was of the order of 1.5 mm/yr. Cooling from ~730°C to ~165°C by 94 Ma is a result of decreased heat flux into the crust and continued exhumation. Rapid cooling accounts for preservation of homogeneous, high-temperature garnet composition profiles and lack of retrogression of high-temperature mineral assemblages [*Smith*, 1992]. An exhumation rate of 1.5 mm/yr is higher than rates estimated for erosional exhumation based on fluvial sediment loads (0.02 to 0.8 mm/yr) [*Young*, 1969, 1971; *Anhert*, 1970] but comparable with rates estimated for exposure of metamorphic rocks in the Alps, Canadian Rocky Mountains and Southern Alps (0.4 to 8 mm/yr) [*Albarède*, 1976; *Clark and Jager*, 1969; *Hollister*, 1979; *Scholz et al.*, 1979]. These comparisons strongly suggest that some tectonic unroofing occurred. Although directly related structures are not exposed, the inferred fault beneath the Balchen Glacier is a likely candidate.

The difference in ages between most of the K-feldspar $^{40}Ar/^{39}Ar$ data (~94 Ma) and the apatite fission track data (~80 Ma) indicates a dramatic slowing of cooling rate after ~94 Ma. Most samples were not cooled completely through the apatite partial annealing zone by ~80 Ma (i.e., to temperatures <60°C), giving rise to the small proportion of shorter tracks. Thus the FMC was not brought completely to the surface as a result of the deformation event associated with initial rapid cooling. However, the dominance of long tracks in the track length distributions and the small standard deviations in all the samples indicate rapid cooling after ~80 Ma. This rapid cooling can be correlated to more rapid exhumation in the FMC, possibly associated with faulting. Without more regional low-temperature cooling data the nature of this final event cannot be determined.

Modeling of the fission track data require that rocks in the FMC were cooled below 60°C by 70 Ma, and thus have been within ~3 km of the surface throughout the Tertiary. It is unknown whether these rocks subsequently were unroofed by continuous slow erosion, perhaps associated with development of an erosion surface similar to a pre-Eocene surface documented in New Zealand [*Le Masurier and Rex*, 1983], or whether there was a more recent rapid exhumation event. Tertiary faulting related to extension in the Ross Sea [*Fitzgerald et al.*, 1986; *Davey*, 1987; *Moore and Ettriem*, 1987; *Stern and ten Brink*, 1989; *Cooper et al.*, 1991] is not responsible for the exhumation of the FMC.

Dynamic Model

The exhumation history of the Fosdick-Chester block was related to distributed deformation in Marie Byrd Land during continental breakup [*Bradshaw*, 1991]. The initial cooling event followed the proposed passage of the subducted remanent of the Pacific-Phoenix ridge (Figure 2) beneath Marie Byrd Land and the resulting transition from active to passive margin in this sector of Gondwana starting at ~105 Ma [*J. D. Bradshaw*, 1989]. The geothermal gradient in the Fosdick Mountains area was strongly elevated by magmatic advection, possibly due to increased mantle heat flux or magmatic underplating (Figure 10) related to the passage of the subducted spreading center. This heating event caused the high-temperature, low-pressure metamorphism in the FMC. Similar metamorphism elsewhere has also been attributed to emplacement of thin, tabular plutons at midcrustal levels [*Lux et al.*, 1986; *DeYoreo et al.*, 1989]. Thermal weakening probably produced a midcrustal asthenospheric environment [*Block and Royden*, 1990; *Kruse et al.*, 1991]. Ensuing deformation (D_3) was probably driven by some combination of gravity potentials resulting from inhomogeneous extension in the upper crust, thinning above a zone of lower crustal magmatic accretion, and penetrative thinning linked with an overlying zone of uniform upper crustal extension.

The final episode of rapid cooling in the FMC, starting at ~80 Ma, was nearly coeval with the initiation of seafloor spreading between the Campbell Plateau and Marie Byrd Land at ~84 Ma [*Christoffel and Falconer*, 1972; *Cande and Mutter*, 1982; *Kamp*, 1986; *Mayes et al.*, 1990]. The N-S extension direction inferred for deformation associated with cooling is strongly oblique to the continental margin of Marie Byrd Land, consistent with a right-shear component during the continental breakup [cf. *Grindley and Davey*, 1982 *Storey*, 1991].

High-grade metamorphism followed by rapid cooling of the FMC shortly before the breakup of Gondwana in this region invites comparison of the FMC with metamorphic core complexes formed in other extensional terranes [*Coney*, 1980; *Davis*, 1980; *Malavieille*, 1993]. The peak metamorphic conditions in the Fosdick Mountains outlasted the ductile deformation event. This contrasts with the structural progression normally observed in crystalline rocks exhumed in the footwall of major normal faults (i.e., metamorphic core complexes), in which ductile deformation is continuous from high-grade to low-grade metamorphic conditions, and late stage brittle faults are superimposed on penetratively deformed rocks [*Lister and Davis*, 1989]. The Fosdick Mountains are not a Cordilleran-style metamorphic core complex, but we interpret that exhumation of the FMC is the result of episodic deformation associated with continental breakup in a complex transtensional environment.

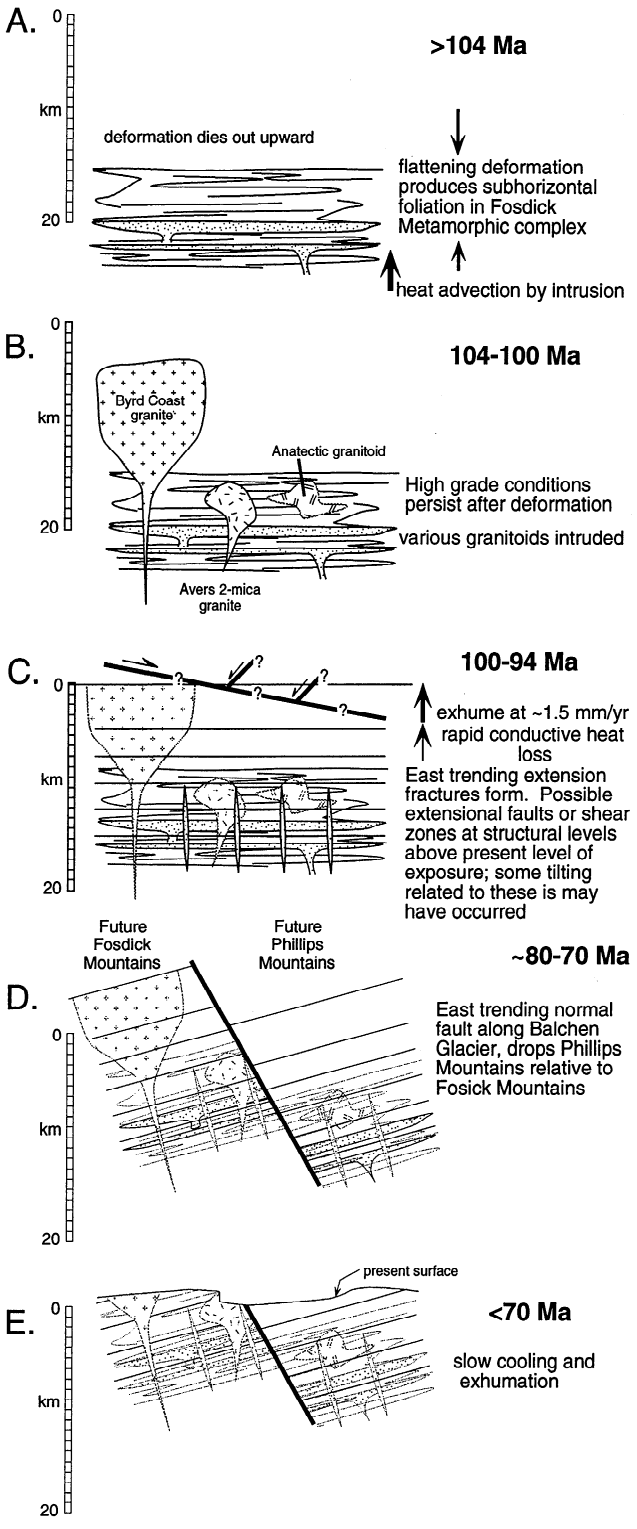

Figure 10. Summary of proposed history. (a) By 104 Ma. magmatic heat advection had resulted in high grade metamorphism, and deformation. (b) Between 104 Ma and 100 Ma the unfoliated Byrd Coast granite and two-mica granite at Mt. Avers granite intruded into already cooling metamorphic rocks. (c) Between 100 Ma and 94 Ma rocks in the FMC underwent significant exhumation and cooled rapidly to ~160°C. Minor structures developed during this period suggest N-S extension. Normal faulting at structural levels above what is presently exposed may have accelerated cooling, and some tilting may have occurred. The cooling rate slowed significantly during the time between ~94 and 80 Ma. (d) Between 80 Ma and 70 Ma normal slip on an east trending normal fault under the Balchen Glacier resulted in tilting of the Fosdick-Chester block and cooling through the apatite fission track partial annealing zone. The FMC had cooled to temperatures <60°C by 70 Ma, at an estimated maximum depth of ~3 km. (e) The history after 70 Ma is characterized by slow cooling and exhumation to the surface. Minor faulting may have occurred during this period.

Appendix: Description of Samples

Descriptions include sample identification used in this paper, followed by sample identification assigned in the field (in parentheses), latitude and longitude and description of sample location, description of rock unit and geologic relationships, and minerals analyzed from the sample. Latitude and longitude were measured on the 1:250,000 Guest Peninsula and Gutenko Nunatak U.S. Geological Survey quadrangles.

Avers 1 (1-1-90-3). 76°27.5'S 145°31.0'W; collected at north end of granitoid body on west side of ridge ~4 km NNW of Mt. Avers. Undeformed, equigranular, fine-grained muscovite-biotite granite. Intrudes FMC, crosscutting gneissic foliation. Sampled for $^{40}Ar/^{39}Ar$ muscovite, biotite, K-feldspar, U-Pb zircon and monazite, and fission track apatite

Birchall (12-24-89-1). 76°26.6'S 146°28.0'W; collected at center of base of cliff on north side of Maigetter Peak. Pegmatitic leucosome crosscutting main gneissic fabric in quartz-feldspar-biotite-sillimanite-garnet gneiss. Pegmatite consisting of coarse-grained quartz, K-feldspar, albite, and minor biotite. Biotite $^{40}Ar/^{39}Ar$.

Bird Bluff 3 (Bird Bluff 3). 76°29.4'S 144°34.0'W; collected from prominent paragneiss layer at base of north end of west facing cliff of eastern summit of Bird Bluff. Paragneiss in FMC. U-Pb monazite.

Chester 1 (Chester 1). 76°38.6'S 145°35.5'W; collected at base of ridge on west side of low saddle in east trending range crest. Ford granodiorite of Chester Mountains; equigranular, medium-grained biotite tonalite. Zircon U-Pb [see *Richard and Kimbrough*, 1991], apatite fission track.

Chester 3 (12-13-89-1). 76°39.5'S 145°29'W; collected from middle dike in swarm of three prominent WNW trending mafic dikes, on west side of bedrock ridge, ~1.2 km south of crest of the range. Dike ~3 m thick; sample collected from core to obtain largest grain size. Consisting of very fine grained plagioclase lathes intergrown with anhedral to subhedral hornblende; hornblende locally altered to actinolite plus chlorite. Tiny nonmagnetic opaque grains and pyrite abundant accessories. Careful density separation used in attempt to concentrate the igneous hornblende for analysis; $^{40}Ar/^{39}Ar$ hornblende to determine crystallization age.

Chester 4 (12-13-89-2). 76°39.1'S 145°29.0'W; collected on west side of crest of bedrock ridge ~0.3 km south of range crest. Porphyritic biotite-muscovite monzogranite that intrudes metasediments in pendant in Ford granodiorite. Rock consisting of ~10% 1-2 cm K-feldspar phenocrysts in a

medium-grained groundmass of ~30% K-feldspar, 20% quartz, 40% plagioclase, and 5-7% biotite and muscovite; $^{40}Ar/^{39}Ar$ muscovite, biotite, K-feldspar.

Corey (Corey 1). 76°39.3'S 145°07.5'W; collected at NW base of Mt. Corey. Byrd Coast granite; equigranular, medium-grained alkali granite. Grades to finer-grained, hypabyssal-looking phase on nunatak just west of Mt. Corey. U-Pb zircon and monazite, fission track apatite.

Getz 1 (1-10-90-3). 76°33.2'S 145°13.7'W; collected on lower part of ridge north of prominent cliff on west face of Mt. Getz. Lineated quartz-hornblende-biotite-plagioclase gneiss, probably a metadiorite, from 10-m-thick concordant lense in gneissic granodiorite; $^{40}Ar/^{39}Ar$ hornblende, biotite.

Getz 2 (1-11-90-2). 76°32.5'S 145°11.0'W; collected from frost-heaved rock in central part of northern summit plateau on Mt. Getz. Anatectic leucogranite (unit 2). Rock consisting of coarse-grained K-feldspar (60%), quartz (20%), and plagioclase (20%), with accessory biotite and garnet. Sillimanite present as inclusions in plagioclase and along fractures. Muscovite appearing secondary, on fractures and disseminated, replacing sillimanite or K-feldspar; $^{40}Ar/^{39}Ar$ muscovite, K-feldspar.

Griffith (GB 2). 76°27.4'S 143°44.0'W; collected on top of small nunatak between two larger of the three Griffiths Nunataks. Weakly foliated, medium-fine-grained, equigranular biotite tonalite. Biotite $^{40}Ar/^{39}Ar$.

Hutcheson (12-3-90-1). 76°17.5'S 143°29.8'W; collected from base of cliff on west side of southern summit of eastern Hutcheson Nunatak. Byrd Coast granite; equigranular, medium-grained alkali granite. U-Pb zircon and monazite, $^{40}Ar/^{39}Ar$ biotite.

June 1 (11-30-90-1). 76°15.7'S 145°04.0'W; collected at east end of low ridge ~2.3 km ESE of Mt. June. Ford granodiorite; equigranular, medium-grained hornblende-biotite tonalite; $^{40}Ar/^{39}Ar$ hornblende.

Lewis 1 (11-28-90-2). 76°17.0'S 145°15.5'S; collected at base of mountain on east side of the NE tip of Lewis Rocks ridge. Fine-grained aplite dike cutting Ford granodiorite; $^{40}Ar/^{39}Ar$ K-feldspar.

Lewis 2 (11-29-90-1). 76°18.4'S 145°23.0W; collected ~1.2 km NE of the SW tip of Lewis Rocks. Sericite-rich selvage along margin of banded quartz vein cutting Ford granodiorite. Drusy quartz lines open-space lenses within the vein. Vein intruding vertical fault striking 055°E; $^{40}Ar/^{39}Ar$ white mica.

Lewis 3 (11-29-90-2). 76°18.6'S 145°23.4'W; collected ~0.75 km NE of the SW tip of Lewis Rocks. Ford granodiorite; equigranular, medium-grained hornblende-biotite tonalite. Minor replacement of hornblende by biotite; $^{40}Ar/^{39}Ar$ biotite

Lockhart 1 (1-2-90-2). 76°26.5'S 145°10.0'W; collected from talus at base of cliff on west side of north trending ridge at the east end of the wind scoop along the northern end of the Mt. Lockhart ridge; ~2 km NW of the summit of Mt. Lockhart. Anatectic leucogranite in FMC (unit 2). Consisting of ~70% coarse-grained K-feldspar, 20% quartz, 5% sericitized plagioclase, and 5% muscovite and biotite; a trace accessory sillimanite present, enclosed in K-feldspar. Muscovite occurring as late magmatic flakes interstitial to quartz and K-feldspar and as secondary flakes with ragged edges replacing K-feldspar and sillimanite. Muscovite also occurring with quartz in microfractures, which in outcrop of similar rocks parallel mesoscopic east trending muscovite-quartz extension fractures; $^{40}Ar/^{39}Ar$ muscovite, K-feldspar.

Lockhart 2 (Lockhart 2). 76°26.5'S 145°11.2'W; collected at base of cliff on north side of NW tip of Mt. Lockhart ridge; ~2.6 km NW of summit of Mt. Lockhart. Equigranular, gneissic garnet monzogranite sill (unit 2) in FMC. U-Pb zircon and monazite, fission track apatite.

Marujupu 1 (Marujupu 2). 76°30.9'S 145°39.0'W; collected on ridge ~20 m above base of granodiorite sheet at southern tip of Marujupu. Foliated granodiorite (unit 2) in FMC. U-Pb zircon and monazite, fission track apatite.

Marujupu 2 (Marujupu 3). 76°31.1'S 145°39.0'W; collected at south tip of Marujupu. Pelitic gneiss in FMC (unit 1). Mineral assemblage including quartz, biotite, sillimanite, garnet, cordierite, and K-feldspar. U-Pb monazite, fission track apatite.

Mutel 1 (MUDUB). 76°31.5'S 146°07.5'W; collected at base of cliff on west side of Mutel Peak. Undeformed mafic dike cutting FMC. Dike consisting of fine-grained hornblende and plagioclase, with abundant accessory acicular apatite. Dike sampled for paleomagnetic analysis; $^{40}Ar/^{39}Ar$ hornblende to establish crystallization age of dike.

Neptune 1 (12-14-89-4). 76°36.6'S 145°17.0'W; collected near NW tip of middle Neptune Nunatak, ~1.5 km ESE of largest (and NW-most) nunatak. Foliated tonalite. Medium grained, equigranular. Consists of quartz, plagioclase, hornblende, and biotite; $^{40}Ar/^{39}Ar$ hornblende and biotite.

Richardson 1a (1-4-90-1). 76°32.7'S 144°41.8'W; collected on south side of ridge extending east from main north trending ridge, ~1 km north of Mt. Richardson summit and 125 m east of main ridge crest. Fine-grained hornblende-biotite-plagioclase metadiorite boudin in quartz-feldspar-biotite orthogneiss. Gneissic internal foliation in boudin slightly discordant to adjacent gneiss. Rock consisting of ~30-40% biotite, 15% hornblende, 25-35% plagioclase, and 15% quartz; apatite an abundant accessory, pyrite present in tiny anhedral crystals. Biotite replacing hornblende; plagioclase slightly to strongly sericitized; biotite locally chloritized but mostly quite fresh; $^{40}Ar/^{39}Ar$ hornblende.

Richardson 1b (1-4-90-2). Same location as Richardson 1a. Quartz-feldspar-biotite gneiss adjacent to boudin of sample Richardson 1a; $^{40}Ar/^{39}Ar$ biotite, K-feldspar.

Richardson 2 (Richardson-2). 76°33.0'S 144°41.9'W; collected on main ridge crest ~300 m north of Mt. Richardson summit. Foliated tonalite, very similar to Marujupu 1. Hornblende replaced entirely by biotite. U-Pb, fission track apatite.

Acknowledgments. Able assistance in the field was provided by A. Cain, J. Roberts, T. Schmidt, and S. Tucker. Special thanks to P. B. Gans for assistance with the $^{40}Ar/^{39}Ar$ analyses. A thorough review by J. D. Bradshaw greatly improved the manuscript. This research was supported by N. S. F. grant DPP 88-17615 (D.L. Kimbrough, B.P. Luyendyk, S.M. Richard, and C.H. Smith), grants DPP 88-16655 and DPP 91-17441 (P.G. Fitzgerald) and DOE DE-FG05-88-ER-75449 (M.O. McWilliams). Institute for Crustal Studies contribution 0085-23CS.

References

Adams, C. J., Geochronological studies of the Swanson Formation of Marie Byrd Land, West Antarctica, and correlation with northern Victoria Land, East Antarctica, and South Island, New Zealand, *N. Z. J. Geol. Geophys., 29,* 345-358, 1986.

Adams, C. J., Geochronology of granite terranes in the Ford Ranges, Marie Byrd Land, West Antarctica, *N. Z. J. Geol. Geophys., 30,* 51-72, 1987.

Adams, C. J., P. Broady, P. J. Cleary, and S. Weaver, Geological and biological expedition to Edward VII peninsula, Marie Byrd Land, West Antarctica-1987/88: Field observations and initial results, *Rep. 9,* pp. 5-34, N. Z. Antarct. Res. Programme, Christchurch, 1989.

Albarède, F., Thermal models of post-tectonic decompression as exemplified by the Haut-Allier granulites (Massif Central, France), *Bull. Geol. Soc. Fr., 18,* 1023-1032, 1976.

Anhert, T., Functional relationship between denudation, relief and uplift in large, mid-latitude drainage basins, *Am. J. Sci., 268,* 243-263, 1970.

Block, L., and L. H. Royden, Core complex geometries and regional-scale flow in the lower crust, *Tectonics, 9,* 557-567, 1990.

Borg, S. G., and D. J. DePaolo, A tectonic model of the Antarctic Gondwana margin with implications for southeastern Australia: Isotopic and geochemical evidence, *Tectonophysics, 196,* 339-358, 1991.

Bradshaw, J. D., Cretaceous dispersion of Gondwana: Continental and oceanic spreading in the south-west Pacific-Antarctic sector, in *Geological Evolution of Antarctica,* edited by M. R. A. Thompson et al., pp. 567-581, Cambridge University Press, New York, 1991.

Bradshaw, J. D., Cretaceous geotectonic patterns in the New Zealand region, *Tectonics, 8,* 803-820, 1989.

Bradshaw, J. D., P. B. Andrews, and B. D. Field, Swanson Formation and related rocks of Marie Byrd Land and a comparison with the Robertson Bay Group of northern Victoria Land, in *Antarctic Earth Science,* edited by R. L. Oliver, pp. 274-279, Canberra, Aust., Australian Academy of Science, 581-585, 1983.

Bradshaw, J. Y., Origin and metamorphic history of an Early Cretaceous polybaric granulite terrain, Fiordland, southwest New Zealand, *Contrib. Mineral. Petrol., 103,* 346-360, 1989.

Cande, S. C., and J. C. Mutter, A revised identification of the oldest sea-floor spreading anomalies between Australia and Antarctica, *Earth Planet. Sci. Lett., 58,* 151-160, 1982.

Christoffel, D. A., and R. H. K. Falconer, Marine magnetic measurements in the southwest Pacific Ocean and the identification of new tectonic features, in *Antarctic Oceanology II: The Australian-New Zealand sector, Antarct. Res. Series,* vol. 19, edited by D. E. Hayes, pp. 197-209, AGU, Washington D. C., 1972.

Clark, S. P., and E. Jager, Denudation rate in the Alps from geochronologic and heat flow data, *Am. J. Sci.,* 267, 1143-1160, 1969.

Coney, P. J., Cordilleran metamorphic core complexes: An overview, in Cordilleran Metamorphic Core Complexes, edited by M. Crittenden, Jr., et al., *Mem. Geol. Soc. Am. 153,* 7-34, 1980.

Cooper, A. K., F. J. Davey, and K. Hinz, Crustal extension and origin of sedimentary basins beneath the Ross Sea and Ross Ice shelf, Antarctica, in *Geological Evolution of Antarctica,* edited by M. R. A. Thomson et al., pp. 285-292, Cambridge University Press, New York, 1991.

Cooper, R. A., C. A. Landis, W. E. LeMasurier, and E. G. Speden, Geologic history and regional patterns in New Zealand and West Antarctica--Their paleotectonic and paleogeographic significance, in *Antarctic Geoscience,* edited by C. Craddock, pp. 43-53, University of Wisconsin Press, Madison, 1982.

Copeland, P., R. R. Parrish, and T. M. Harrison, Identification of inherited radiogenic Pb in monazite and its implications for U-Pb systematics, *Nature, 333,* 760-763, 1988.

Crowley, K. D., Neutron dosimetry in fission-track analysis, *Nucl. Tracks Radiat. Meas., 11,* 237-243, 1986.

Dalrymple, G. B., and M. A. Lanphere, *Potassium-Argon Dating,* 258 pp., W. H. Freeman, New York, 1969.

Dalziel, I. W. D., and R. L. Brown, Tectonic denudation of the Darwin metamorphic core complex in the Andes of Tierra del Fuego, southernmost Chile: Implications for Cordilleran orogenesis, *Geology, 17,* 699-703, 1989.

Dalziel, I. W. D., and D. H. Elliot, West Antarctica: Problem child of Gondwana, *Tectonics, 1,* 3-19, 1982.

Dalziel, I. W. D., and A. Grunow, The Pacific margin of Antarctica: Terranes within terranes within terranes, in *Circum-Pacific Terranes, Earth Sci. Ser.,* vol. 1, edited by D. G. Howell, pp. 555-564, Circum-Pac. Counc. for Energy and Miner. Resourc., Houston, Tex., 1985.

Dalziel, I. W. D., B. C. Storey, S. W. Garrett, A. M. Grunow, L. D. B. Herrod, and R. J. Pankhurst, Extensional tectonics and the fragmentation of Gondwanaland, in Continental Extensional Tectonics, edited by J. F. Dewey et al., *Geol. Soc. Spec. Publ. London, 28,* 433-441, 1987.

Davey, F. J., Geology and structure of the Ross Sea region, in *The Antarctic Continental Margin: Geology and Geophysics of the Western Ross Sea, Earth Sci. Ser.,* vol 5B, edited by A. K. Cooper et al., pp. 1-15, Circum-Pac. Counc. for Energy and Miner. Resour., Houston, Tex., 1987.

Davis, G. A., and G. S. Lister, Detachment faulting in continental extension: Perspectives from the southwestern U. S. Cordillera, in Processes in Continental Lithospheric Deformation, edited by S. P. Clark, Jr., et al., *Spec. Pap. Geol. Soc. Am, 218,* 133-160, 1988.

Davis, G. H., Structural characteristics of metamorphic core complexes, southern Arizona, in Cordilleran Metamorphic Core Complexes, edited by M. Crittenden, Jr., et al., *Mem. Geol. Soc. Am., 153,* 35-77, 1980.

DeWit, M. J., Gondwana research; New breakthrough, old supercontinent, *S. Afr. J. Earth Sci., 86,* 479-483, 1990.

DeYoreo, J. J., D. R. Lux, and C. V. Guidotti, The role of crustal anatexis and magma migration in the thermal evolution of regions of thickened continental crust, in Evolution of Metamorphic Belts, edited by J. S. Daley et al., *Geol. Soc. Spec. Publ., London, 43,* 187-202, 1989.

Dodson, M. H., Closure temperature in cooling geochronological and petrological systems, *Contrib. Miner. Petrol.,* 40, 259-274, 1973.

England, P. C., and A. B. Thompson, Pressure-temperature-time paths of regional metamorphism., I, Heat transfer during the evolution of regions of thickened continental crust, *J. Petrol., 25,* 894-928, 1984.

Fitzgerald, P. G., M. Sandiford, P. J. Barrett, and A. J. W. Gleadow, Asymmetric extension associated with uplift and subsidence in the Transantarctic Mountains and Ross Embayment, *Earth Planet. Sci. Lett., 81,* 67-78, 1986.

Galbraith, R. F., On statistical models of fission track counts, *J. Int. Assoc. Math. Geol., 13,* 471-478, 1981.

Ganguly, J., and S. K. Saxena, Mixing properties of alumino-silicate garnets, constraints from natural and experimental data, and applications to geothermobarometry, *Am. Mineral., 69,* 88-97, 1984.

Gibson, G. M., I. McDougall, and T. R. Ireland, Age constraints on metamorphism and the development of a metamorphic core complex in Fiordland, southern New Zealand, *Geology, 16,* 405-408, 1988.

Green, P. F., A new look at statistics in fission track dating, *Nucl. Tracks,* 5, 77-86, 1981.

Green, P. F., On the thermotectonic evolution of Northern England: Evidence from fission track analysis, *Geol. Mag.,* 123, 493-506, 1986.

Green, P. F., I. R. Duddy, A. J. W. Gleadow, P. T. Tingate, and G. M. Laslett, Thermal annealing of fission tracks in apatite, 1, A qualitative description, *Isot. Geosci., 59,* 237-253, 1986.

Green, P. F., I. R. Duddy, G. M. Laslett, K. A. Hegarty, A. J. W. Gleadow, and J. F. Lovering, Thermal annealing of fission tracks in apatite, 4, Quantitative modeling techniques and extension to geological timescales, *Isot. Geosci., 79,* 155-167, 1989.

Grindley, G. W., and F. J. Davey, The reconstruction of New Zealand, Australia and Antarctica, in *Antarctic Geoscience,* edited by C. Craddock, pp. 15-29, University of Wisconsin Press, Madison, 1982.

Haller, J., *Geology of East Greenland Cale-*

donides, 413 pp., Wiley-Interscience, New York, 1971.

Halpern, M., Ages of Antarctic and Argentine rocks bearing on continental drift, *Earth Planet. Sci. Lett.*, 5, 159-167, 1968.

Halpern, M., Rb-Sr total-rock and mineral ages from the Marguerite Bay area, Kohler Range and Fosdick Mountains, in *Antarctic Geology and Geophysics*, edited by R. J. Adie, pp. 197-204, Universitetsforlaget, Oslo, 1972.

Harrison, T. M., and J. D. FitzGerald, Exsolution in hornblende and its consequences for ^{40}Ar-^{39}Ar age spectra and closure temperature, *Geochim. Cosmochim. Acta, 50*, 247-253, 1986.

Hollister, L. S., Metamorphism and crustal displacements, *Episodes, 10*, 1979, 3-8, 1979.

Hurford, A. J., and P. F. Green, The zeta age calibration of fission track dating, *Isot. Geosci., 1*, 285-317, 1983.

Kamp, P. J. J., Late Cretaceous-Cenozoic tectonic development of the southwest Pacific, *Tectonophysics, 121*, 225-251, 1986.

Kamp, P. J. J., and P. G. Fitzgerald, Geologic constraints on the Antarctica-Australia-Pacific relative plate motion circuit, *Geology, 15*, 694-697, 1987.

Kimbrough, D. L., B. P. Luyendyk, S. M. Richard, and C. H. Smith, Geology of metamorphic rocks and granitoids: Ford Ranges of western Marie Byrd Land, *Antarct. J. U. S., 25*, 3-5, 1990.

Klimov, L. V., Some results of geological observations in Marie Byrd Land, 1966-1967 (in Russian), *Inf. Byull. Sov. Antark. Eksped., 66*, 18-25, 1967. (*Sov. Antarct. Exp. Inf. Bull., Engl. Transl., 6*, (6), 555-559, 1967.)

Koziol, A. M., and R. C. Newton, Redetermination of the anorthite breakdown reaction and improvement of the plagioclase-garnet-Al_2SiO_5-quartz geobarometer, *Am. Mineral., 73*, 216-223, 1988.

Kruse, S., M. McNutt, J. Phipps-Morgan, L. Royden, and B. Wernicke, Lithospheric extension near Lake Mead, Nevada: A model for ductile flow in the lower crust, *J. Geophys. Res., 96*, 4435-4456, 1991.

Laslett, G. M., A. J. W. Gleadow, and I. R. Duddy, The relationship between fission track length and density in apatite, *Nucl. Tracks Radiat. Meas., 9*, 29-38, 1984.

Laslett, G. M., P. F. Green, I. R. Duddy, and A. J. W. Gleadow, Thermal annealing of fission tracks in apatite, 2, A quantitative analysis, *Isot. Geosci., 65*, 1-13, 1987.

Lawver, L. A., and L. M. Gahagan, Constraints on Mesozoic transtension in Antarctica (abstract), in *Abstracts, Sixth International Symposium on Antarctic Earth Sciences*, pp. 343-344, National Institute of Polar Research, Tokyo, Japan, 1991.

Lawver, L. A., and C. R. Scotese, A revised reconstruction of Gondwanaland, in *Gondwana Six: Structure, Tectonics, and Geophysics, Geophys. Monogr. Ser.*, vol. 40, edited by G. D. McKenzie, pp. 17-24, AGU, Washington D. C., 1987.

Lawver, L. A., J. G. Sclater, and L. Meinke, Mesozoic and Cenozoic reconstruction of the South Atlantic, *Tectonophysics, 114*, 233-54, 1985.

Lawver, L. A., J. Y. Royer, D. T. Sandwell, and C. R. Scotese, Evolution of the Antarctic continental margin, in *Geological Evolution of Antarctica*, edited by M. R. A. Thomson et al., pp. 533-539, Cambridge University Press, New York, 1991.

Le Masurier, W. E., and D. C. Rex, Rate of uplift and the scale of ice level instabilities recorded by volcanic rocks in Marie Byrd Land, West Antarctica, in *Antarctic Earth Science*, edited by R. L. Oliver et al., pp. 663-670, Australian Academy of Science, Canberra, Aust. Capital Territ., 1983.

Lister, G. S., and G. A. Davis, The origin of metamorphic core complexes and detachment faults formed during Tertiary continental extension in the northern Colorado River region, U. S. A., *J. Struct. Geol., 11*, 65-94, 1989.

Lopatin, B. G., and E. M. Orlenko, Outline of the geology of Marie Byrd Land and the Eights Coast, in *Antarctic Geology and Geophysics*, edited by R. J. Adie, pp. 245-250, Universitetsforlaget, Oslo, 1972.

Lovera, O. M., F. M. Richter, and T. M. Harrison, The $^{40}Ar/^{39}Ar$ thermochronometry for slowly cooled samples having a distribution of diffusion domain sizes, *J. Geophys. Res.*, 94, 17,917-17,935, 1989.

Ludwig, K. L., PBDAT for MS-DOS, a computer program for IBM PC compatibles for processing raw U-Th-Pb isotope data, version 1.05, revised April 1989, *U. S. Geol. Surv. Open file report 88-542*, 39 pp., 1989.

Lux, D. R., J. J. DeYoreo, C. V. Guidotti, and E. R. Decker, Role of plutonism in low-pressure metamorphic belt formation, *Nature, 323*, 794-796, 1986.

Luyendyk, B. P., Crustal extension, the exhumation of mid-crustal rocks, and the formation of basin-and-range structure in the northern Edsel Ford Ranges, western Marie Byrd Land, West Antarctica, *Annali di Geofisica*, 36: 165-177, 1993.

Luyendyk, B. P., S. M. Richard, C. H. Smith, and D. L. Kimbrough, Geological and geophysical investigations in the northern Ford Ranges, Marie Byrd Land, West Antarctica, *Antarct. J. U. S., 26*, 67-69, 1991.

Luyendyk, B. P., S. M. Richard, C. H. Smith, and D. L. Kimbrough, Geological and geophysical investigations in the northern Ford Ranges, Marie Byrd Land, West Antarctica, in *Recent Progress in Antarctic Earth Science*, edited by Y. Yoshida et al., pp. 279-288, Terrapub, Tokyo, 1992.

Malavieille, J., Late orogenic extension in mountain belts: Insights from the Basin and Range and the Late Paleozoic Variscan belt, *Tectonics, 12*, 1115-1130, 1993.

Mattinson, J. M., D. L. Kimbrough, and J. Y. Bradshaw, Western Fiordland orthogneiss: Early Cretaceous arc magmatism and granulite facies metamorphism, New Zealand, *Contrib. Mineral. Petrol., 92*, 383-392, 1986.

Mayes, C. L., L. A. Lawver, and D. T. Sandwell, Tectonic history and new isochron chart of the South Pacific, *J. Geophys. Res., 95*, 8543-8567, 1990.

McDougall, I., and T. M. Harrison, *Geochronology and Thermochronology by the $^{40}Ar/^{39}Ar$ Method*, 212 pp., Oxford University Press, New York, 1988.

Mezger, K., C. M. Rawnsley, S. R. Bohlen, and G. N. Hanson, U-Pb garnet, sphene, monazite, and rutile ages: Implications for the duration of high-grade metamorphism and cooling histories, Adirondack Mountains, New York, *J. Geol., 99*, 415-428, 1991.

Moore, G. W., and S. L. Ettriem, Mechanism of extension and rifting at the Antarctic continental margin, in *The Antarctic Continental Margin: Geology and Geophysics of Offshore Wilkes Land, Earth Sci. Ser.*, vol . 5A, edited by S. L. Eittreim et al., pp. 89-98, Circum-Pac. Counc. for Energy and Miner. Resour., Houston, Tex., 1987.

Mukasa, S. B.,I. W. D. Dalziel, and H. K. Brueckner, Zircon U-Pb constraints on the kinematic evolution of the northern Scotia Arc (abstract), *Geol. Soc. Am. Abstr. Programs, 20*(7), A12, 1988.

Newton, R. C., and H. T. Haselton, Thermodynamics of the garnet-plagioclase-Al_2SiO_5-quartz geobarometer, in *Thermodynamics of Minerals and Melts*, edited by R. C. Newton et al., pp. 131-147, Springer-Verlag, New York, 1981.

Parrish, R. R., U-Pb systematics of monazite and its closure temperature based on natural examples (abstract), *Geol. Assoc. Can. Abstr. Program, 13*, A94, 1988.

Peacock, S. M., Thermal modeling of metamorphic pressure-temperature-time paths: A forward approach, in *Metamorphic Pressure-Temperature-Time Paths, Short Course Geol. Ser.*, vol. 7, edited by F. S. Spear and S. M. Peacock, pp. 57-102, AGU, Washington, D. C., 1989.

Peacock, S. M., Numerical simulation of regional and contact metamorphism on the MacIntosh microcomputer, *J. Geol. Educ., 38*, 132-137, 1990.

Richard, S. M., Structure and cooling history of the Fosdick Metamorphic complex, Marie Byrd Land, west Antarctica, in *Recent Progress in Antarctic Earth Science*, edited by Y. Yoshida et al., pp. 289-294, Terrapub, Tokyo, 1992.

Richard, S. M., and D. L. Kimbrough, Mesozoic plutonism, metamorphism of Paleozoic rocks, and cooling related to Gondwana rifting, Fosdick Mountains region, West Antarctica (abstract), *Geol. Soc. Am. Abstr. Programs, 23*(5), A364, 1991.

Schärer, U., The effect of initial ^{230}Th disequilibrium on young U-Pb ages: The Makalu case, Himalaya, *Earth Planet. Sci. Lett., 67*, 191-204, 1984.

Scholz, C. H., J. Beavan, and T. C. Hanks, Frictional metamorphism, argon depletion, and tectonic stress on the Alpine Fault, New Zealand, *J. Geophys. Res., 84*, 6770-6782, 1979.

Smith, C. H., Migmatites at the amphibolite-granulite transition, Fosdick Metamorphic Complex, West Antarctica, in *Recent Pro-*

gress in Antarctic Earth Science, edited by Y. Yoshida et al., pp. 295-301, Terrapub, Tokyo, 1992.

Spear, F. S., Metamorphic fractional crystallization and internal metasomatism by diffusional homogenization of zoned garnets, *Contrib. Mineral. Petrol., 99*, 507-517, 1988.

Stacey, J. S., and J. D. Kramers, Approximation of terrestrial lead isotope evolution by a two-stage model, *Earth Plan. Sci. Lett., 26*, 207-221, 1975.

Stern, T. A., and U. S. ten Brink, Flexural uplift of the Transantarctic Mountains, *J. Geophys. Res., 94*, 10,315-10330, 1989.

Storey, B. C., The crustal blocks of West Antarctica within Gondwana: Reconstruction and break up model, in *Geological Evolution of Antarctica*, edited by M. R. A. Thomson et al., pp. 587-592, Cambridge University Press, New York, 1991.

Storey, B. C., M. J. Hole, R. J. Pankhurst, I. L. Millar, and W. Vennum, Middle Jurassic within-plate granites in West Antarctica and their bearing on the break-up of Gondwanaland, *J. Geol. Soc. London, 145*, 999-1007, 1988.

Stump, E., A. J. R. White, and S. G. Borg, Reconstructions of Australia and Antarctica: Evidence from granites and recent mapping, *Earth Planet. Sci. Lett., 79*, 348-360, 1986.

Tracy, R. J., Compositional zoning and inclusions in metamorphic minerals, in Characterization of Metamorphism Through Mineral Equilibria, edited by J. M. Ferry, *Rev. Mineral., 10*, 355-397, 1982.

Tulloch, A. J., and D. L. Kimbrough, The Paparoa metamorphic core complex, New Zealand: Cretaceous extension associated with fragmentation of the Pacific margin of Gondwana, *Tectonics, 8*, 1217-1234, 1989.

Wade, F. A., and D. R. Couch, The Swanson Formation, Ford Ranges, Marie Byrd Land, Evidence for and against a direct relationship with the Robertson Bay Group, northern Victoria Land, in *Antarct. Geosci., Symp. Antarct. Geol. Geophys., 3rd, 1977*, edited by C. Craddock, pp. 609-618, University of Wisconsin Press, Madison, 1982.

Wade, F. A., and T. R. Wilbanks, Geology of Marie Byrd and Ellsworth Lands, in *Antarct. Geology and Geophysics*, edited by R. J. Adie, pp. 207-214, Universitetsforlaget, Oslo, 1972.

Wade, F. A., C. A. Cathey, and J. B. Oldham, Reconnaissance geologic map of the Boyd Glacier quadrangle, Marie Byrd Land, Antarctica, scale 1:250,000, *Antarct. Geol. Map A-6*, U. S. Geol. Surv., Reston, Va., 1977a.

Wade, F. A., C. A. Cathey, and J. B. Oldham, Reconnaissance geologic map of the Alexandra Mountains quadrangle, Marie Byrd Land, Antarctica, scale 1:250,000, *Antarct. Geol. Map A-5*, U. S. Geol. Surv., Reston, Va., 1977b.

Wade, F. A., C. A. Cathey, and J. B. Oldham, Reconnaissance geologic map of the Guest Peninsula quadrangle, Marie Byrd Land, Antarctica, scale 1:250,000, *Antarct. Geol. Map A-7*, U. S. Geol. Surv., Reston, Va., 1977c.

Wade, F. A., C. A. Cathey, and J. B. Oldham, Reconnaissance geologic map of the Gutenko Nunataks quadrangle, Marie Byrd Land, Antarctica, scale 1:250,000, Prog. *Antarct. Geol. Map A-11*, U. S. Geol. Surv., Reston, Va., 1978.

Weaver, S. D., J. D. Bradshaw, and C. J. Adams, Granitoids of the Ford Ranges, Marie Byrd Land, Antarctica, in *Geological Evolution of Antarctica*, edited by M. R. A. Thomson et al., pp. 345-352, Cambridge University Press, New York, 1991.

Weaver, S. D., C. J. Adams, R. J. Pankhurst, and I. L. Gibson, Granites of Edward VII Peninsula, Marie Byrd Land: Anorogenic magmatism related to Antarctic-New Zealand rifting, *Trans. R. Soc. Edinburgh Earth Sci., 83*, 281-290, 1992.

Wilbanks, J. R., Geology of the Fosdick Mountains, Marie Byrd Land, West Antarctica, Ph. D. dissertation, 219 pp., Tex. Tech. Coll., Lubbock, 1969.

Wilbanks, J. R., Geology of the Fosdick Mountains, Marie Byrd Land, in *Antarctic Geology and Geophysics*, edited by R. J. Adie, pp. 277-284, Universitetsforlaget, Oslo, 1972.

Young, A., Present rate of land erosion, *Nature, 224*, 851-852, 1969.

Young, A., Rate of slope retreat, in Slopes, Form and Process, edited by D. Brunsden, *Spec. Publ. 3*, 65-78, Inst. Brit. Geogr., London, 1971.

Zeitler, P. K., Argon diffusion in partially outgassed alkali feldspars: Insights from ^{40}Ar-^{39}Ar analysis, *Isot. Geosci., 65*, 167-181, 1987.

Zen, E., Evidence for accreted terranes and the effect of metamorphism, *Am. J. Sci., 288A*, 1-15, 1988.

Zen, E., Using granite to image the thermal state of the source terrane, *Trans. R. Soc. Edinburgh, 83*, 107-114, 1992.

P. G. Fitzgerald, Geosciences Department, University of Arizona, Tucson, AZ 85721. (e-mail: Kiwi@sapphire.geo.arizona.edu)

D. L. Kimbrough, Department of Geological Sciences, San Diego State University, San Diego, CA 92182. (e-mail: Kimbrough-@ucsvax.sdsu.edu)

B. P. Luyendyk, Institute for Crustal Studies, University of California, Santa Barbara, CA 93106. (e-mail: Luyendyk@quake.-crustal.ucsb.edu)

M. O. McWilliams, Department of Geophysics, Stanford University, Stanford, CA 94305. (e-mail: Mac@pangea.Stanford.edu)

S. M. Richard, Arizona Geological Survey, 845 North Park Avenue, #100, Tucson, AZ, 85719. (e-mail: Srichard@ccit.Arizona.edu)

C. H. Smith, Geology Department, Colorado College, Colorado Springs, CO 80903. (e-mail: Chsmith@ccnode.Colorado.edu)

(Received June 4, 1993; revised November 22, 1993; accepted November 26, 1993)